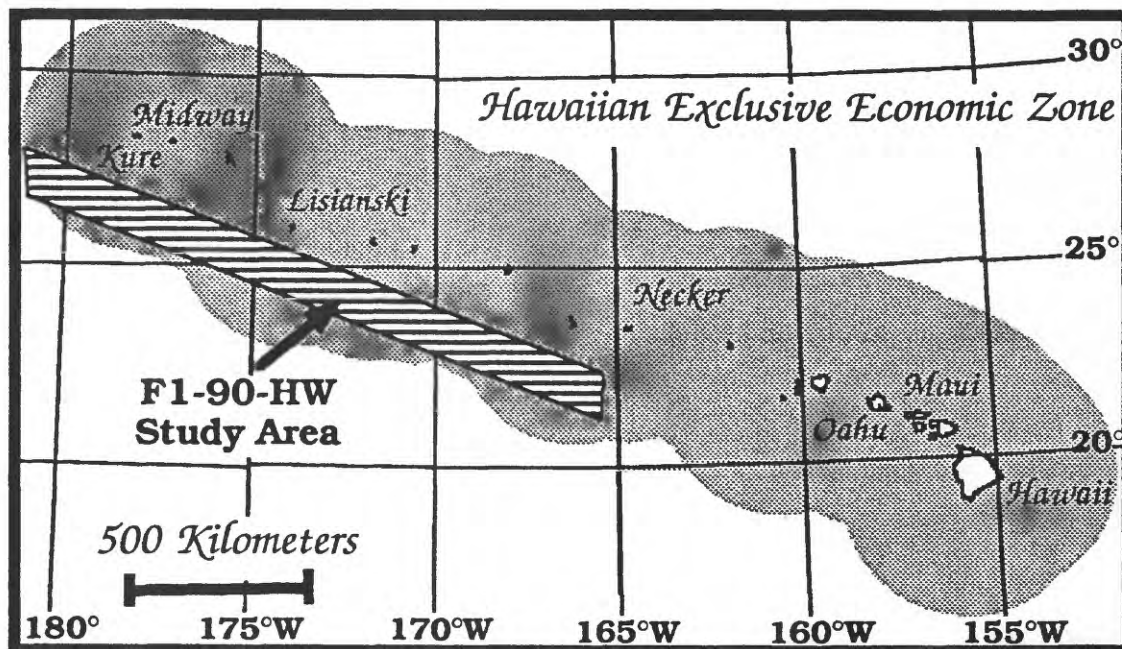


Department of the Interior  
U.S. Geological Survey

Cruise Report:  
GLORIA Survey of Part of the Hawaiian Exclusive Economic Zone,  
F1-90-HW



by

Robert E. Kayen<sup>1</sup>, Monty A. Hampton<sup>1</sup>, John B. Wilson<sup>2</sup>, and Derek G. Bishop<sup>2</sup>

Open-File Report 90-345

July, 1990

<sup>1</sup>U.S. Geological Survey, Menlo Park, CA 94025

<sup>2</sup>IOSDL, Wormley, Godalming, Surrey, United Kingdom

This report is preliminary and has not been reviewed for conformity with U.S. Geological Survey editorial standards. Any use of trade, product, or firm is for descriptive purposes only and does not imply endorsement by the U.S. Government.

## Summary of Scientific Results

Cruise F1-90-HW is part of the cooperative United States Geological Survey (USGS) /British Institute of Oceanographic Sciences (IOS), project to map the seafloor of the U.S. Exclusive Economic Zone (EEZ) at a reconnaissance scale using the GLORIA (Geological Long-Range Inclined Asdic) side-scanning sonar system and acoustic-reflection profilers. Cruise F1-90-HW was one of three consecutive cruises whose survey area covers the EEZ south of the Hawaiian island chain from Necker Ridge to 320 km beyond Kure Island (Figure 1). The results presented herein were derived from shipboard observations of the GLORIA images and acoustic-reflection profiles and should be regarded as preliminary.

### Cretaceous Seafloor

The seafloor in the study area was formed approximately between 95 and 128 Ma at the East Pacific Rise, largely during the Cretaceous magnetic quiet zone (Atwater, 1989). Characteristic linear seafloor fabric from the horst and graben structure of the oceanic crust can be seen clearly in GLORIA images from the western portion of the survey area where local uplift or large fault offset has caused seafloor topographic expression of the ridge-crests. Spreading fabric on this portion of the seafloor strikes N20W. The faults are spaced 1.5 to 5 km apart and can be traced obliquely across the width of the study area, over 160 kilometers. Backscatter variations that manifest the fabric probably are not associated directly with the topographic relief of the horsts, but instead are due to the presence of

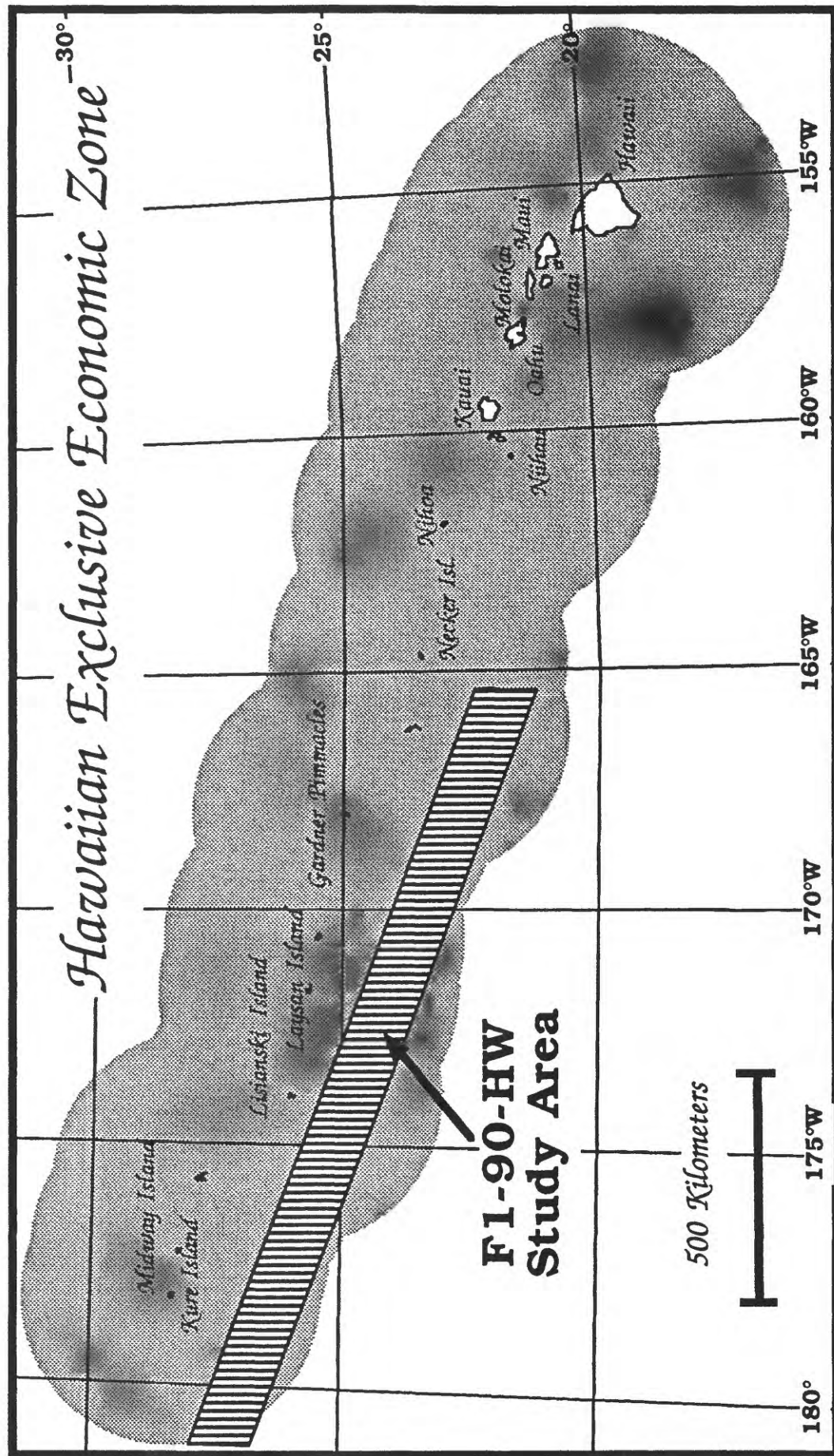


Figure 1. Location map of the Hawaiian Island EEZ and study area of F1-90-HW.

buried, strongly backscattering sediment layers within the sediment drape above the graben. Volcanic ridges and seamounts that trend parallel to the spreading fabric indicate the structural grain elsewhere, but in most places the basement fabric is masked by a relatively thick sediment drape.

(Several?) Transform faults that cross the study area with a strike of N65E are visible at the seafloor where sediment cover is thin, or where volcanic features occur above leaky segments of the faults. In particular, five lineations are interpreted as part of the Murray Fracture Zone (MFZ), a large transform fault zone that extends east to near the United States mainland. Lineated volcanic features along the MFZ appear to have issued from the faults themselves. The MFZ extends in an echelon fashion to the middle section of the adjacent study area to the south, insonified previously during F13-89-HW. Measurements suggest that the MFZ is as much as 150 km wide within the two survey areas and is defined by as many as seven faults. A fault parallel to and west of the MFZ truncates and bends the seafloor spreading fabric. The direction of bending clearly indicates a left-lateral (sinistral) sense of motion.

Four types of Cretaceous(?) seamounts were observed during the survey: I) small and smooth-surfaced, circular, low-relief seamounts with or without a summit crater and commonly having a conspicuous halo of high backscatter; II) large (>10 km across) rough-surfaced and possibly degraded, non-circular seamounts; III) small (5-10 km across) rough-surfaced and possibly degraded, non-circular seamounts; IV) very small (less than 2 km across) rough-surfaced volcanic mounds or spatter cones.

A group of Type-II volcanoes and guyots in the central portion of the study area is highly degraded by debris avalanching and gullying. This cluster of seamounts is adjacent to the Hawaiian Ridge and therefore is

likely to have been exposed to environmental stresses in excess of those felt by other abyssal seamounts in the Mid-Pacific Mountains. These stresses include earthquake loading, crustal subsidence and arching across the main axis of the ridge, and partial volcanic overprinting by the propagating Hawaiian hot spot.

The eastern portion of the survey area is crossed by the Necker Ridge of Cretaceous Age, which appears to have formed by massive eruptions along a leaky transform-fault trending N48E. Two subsidiary ridges, parallel and west of Necker Ridge, were observed 45 and 90 km to the northwest.

An elongate sheet flow at least 800 km<sup>2</sup> in area was insonified near a large Type II volcano at 173° 45'W, 26° 20'N and apparently flowed downslope to the south for at least 65 km. However, the flow is nowhere more than 10 km wide. The sheet flow is interpreted to have been of low viscosity. Acoustic-reflection profiles across the flow indicate that it lies within a topographic low, and it is characterized by opaque, and characteristically weak, "mushy" reflections.

### Sedimentary Features

A sequence of horizontal reflectors more than 0.6 sec (two-way travel time in reflection profiles) thick in places covers oceanic basement. The reflector sequence has a basin-fill pattern and probably is composed of turbidites. The high-resolution profiles show an acoustically transparent layer, in places containing one or more "hard" reflectors and reaching a thickness of up to 0.050 sec, that drapes the seafloor except on the steep flanks of some seamounts.

Sediment-draped seafloor in GLORIA images has a range of backscatter intensities that is in most places determined by penetration of acoustic energy beneath the seafloor and attenuated backscatter off buried features. Where the transparent drape is greater than about 0.025 sec thick and without internal hard reflectors, backscatter is weak, but where the drape is thinner, especially where the underlying material is hard or rough, or where the drape contains shallow hard reflectors, the backscatter is relatively strong.

A submarine valley system at 172° 35'W, 23° 55'N has at least two tributary channels that coalesce and apparently funnel sediment to a depocenter southeast of the study area in a region insonified during F13-89-HW. Topographic relief across the channel is less than 8 meters.

### Mass Wasting Features

The distal end of a giant debris avalanche was insonified at 174° 45'W, 25° 25'N and appears to have flowed southwest from the slopes of Lisianski Island and Neva shoal, approximately 90 km upslope from the toe of the slide. The toe is characterized by large isolated blocks as much as 1 km long. The long distance of travel and the isolated-blocky nature of the slide suggest that it moved rapidly downslope.

A number of large, rough-surfaced seamounts have what appear to be gullies, debris chutes, amphitheaters, and debris avalanche deposits.

These features suggest that mass-wasting is an important component affecting the morphologic evolution of the seamounts.

## INTRODUCTION

Cruise F1-90-HW was the tenth cruise of the multi-year cooperative program between the United States Geological Survey (USGS) and the British Institute of Oceanographic Sciences (IOS) to map the seafloor of the Hawaii Exclusive Economic Zone. The primary objective of the program is to produce total-coverage, mosaic maps of the seafloor within the Hawaii EEZ using acoustically derived images from the GLORIA long-range side-scanning sonar system.

Cruise F1-90-HW was the second of three consecutive surveys of the EEZ south of the Hawaiian Ridge, between Nihoa Island and 320 km west of Kure Island (Figure 1). The previous cruise, F13-89-HW, conducted in November and December, 1989, surveyed the outer portion of the EEZ, and the following cruise F2-90-HW will survey the inner portion, directly south of the Hawaiian chain. Thirteen tracklines were run during F1-90-HW to survey the intervening portion of the EEZ (Figure 2). This series of three cruises is adjacent and west of the area surveyed by F10-88-HW (McGregor et al., 1989). The remaining northern waters of the Hawaiian EEZ are scheduled to be surveyed in 1991.

Operations on-board the R/V Farnella included the collection of a variety of geophysical and acoustic data, including GLORIA long-range, dual channel, side-scan sonar images; two-channel seismic-reflection profiles using a 2620 cm<sup>3</sup> (160 in<sup>3</sup>) air-gun sound source, 3.5-kHz high-

resolution profiles, 10-kHz bathymetric profiles, magnetic- and gravity-field records, and upper water-column temperature profiles using expendable bathythermographs (XBTs).



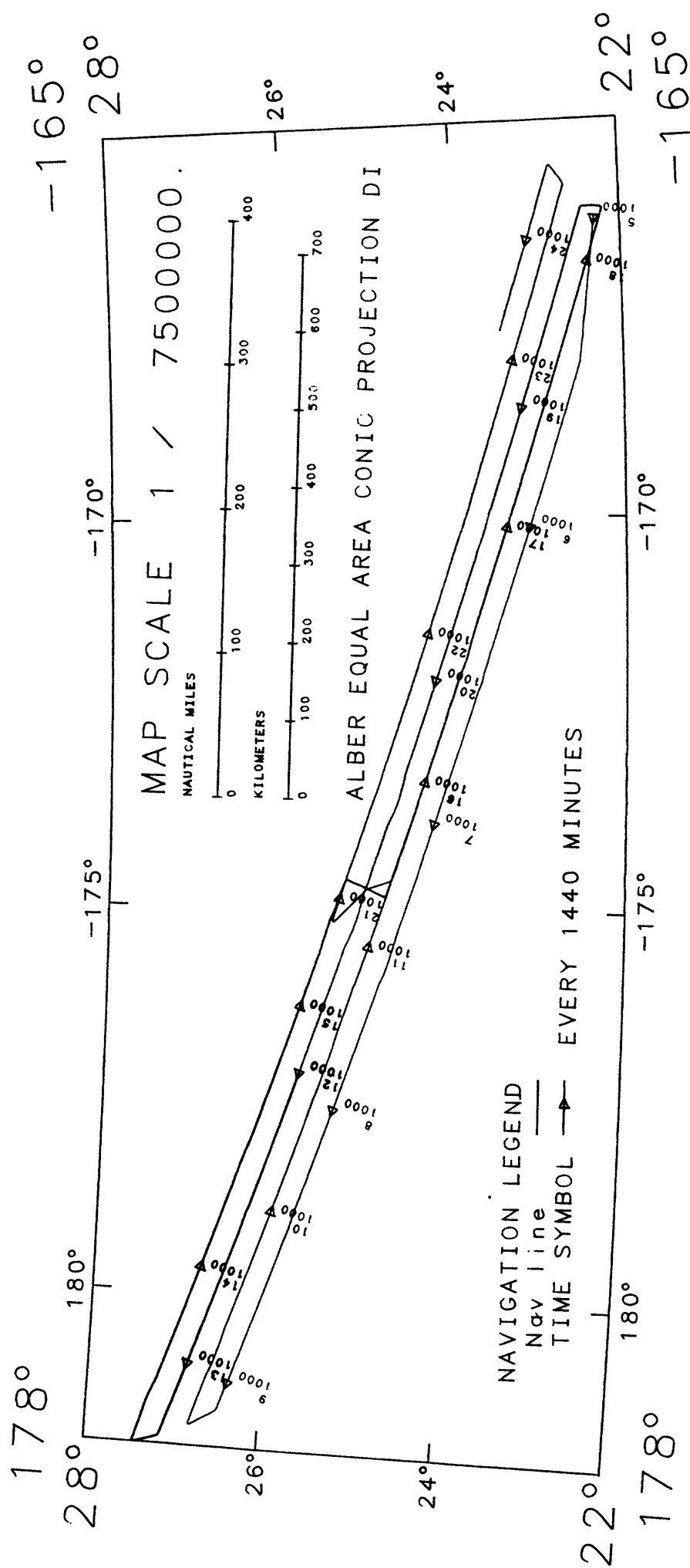


Figure 2. Trackline plot of the R.V. Farnella during F1-90-HW field operations (scale 1:7,500,000).

## SCIENTIFIC STAFF FOR F1-90-HW

### *U.S. Geological Survey*

Monty A. Hampton	Co-chief Scientist - Geologist
Robert E. Kayen	Co-chief Scientist - Civil Engineer
Kaye Kinoshita	Navigator - Watchstander
Grace Fong	Data archivist - Watchstander
Matthew Morgan	Watchstander
Jim Vaughan	Electronic Engineer

### *Institute of Oceanographic Sciences, U.K.*

John Wilson	Co-chief Scientist - Geologist
Derek Bishop	GLORIA Engineer
Jon Campbell	GLORIA Engineer
Andrew Webb	Mech. Engineer

### *Research Vessel Services (RVS), Barry, U.K.*

David Beasley	Navigator
---------------	-----------

### *JMarr (Ships Crew)*

Ronald Holliday	Captain
Albert Fuller	Chief Officer
David Shaw	2nd Officer
Michael Baldwin	Chief Engineer
David Rogerson	2nd Engineer
Arthur Green	3rd Engineer
Robin Searle	Electrician
Alan Thompson	Bosun
Jimmy Springall	Seaman
Peter Appleyard	Seaman
Michael Jessop	Seaman

Thomas Caughie	Chief Cook
Pat Fitzgerald	Second Cook
David Graves	Steward

### **Summary of Field Operations**

The R/V Farnella was used as the research platform for conducting the seafloor mapping surveys. The Farnella is under lease to the U.S. Geological Survey through the British Institute of Oceanographic Sciences (IOS), Wormley, England. IOS personnel were responsible for operations involving the GLORIA system and GLORIA image production. IOS also was in charge of scientific deck operations and maintenance of geophysical equipment. Acquisition and processing of navigation data were performed by both USGS and RVS personnel. The USGS personnel monitored the gravimeter, magnetometer, acoustic-reflection, 3.5 kHz and 10 kHz recording systems. The co-chief scientists coordinated and supervised cruise planning and shipboard operations. Additionally, co-chief scientists produced three GLORIA field mosaics and this preliminary shipboard science report.

The following cruise calendar is presented in Julian Day/Greenwich Mean Time (GMT), for major operations of F1-90-HW. In order to convert to local Hawaiian time, subtract 10 hours from GMT. The Julian day 001 refers to January 1. Figure 1 provides a geographic reference for the region covered by this survey, and Figure 2 is a trackline summary to provide a reference for the progress of the survey.

The survey originally was planned to be run along 4 long lines oriented parallel to the Hawaiian Ridge, with short, orthogonal connecting lines. However, weather conditions necessitated completion of the coverage in the western third of the area before proceeding on to the eastern two-thirds. The survey was finished with an additional day of ship time, and as such, we ran fourteen hours of trackline scheduled for F2-90-HW. (Note: SOL=start of line, EOL=end of line.)

#### Day 003

- 0200; Gravity tie #1 reading at the Bishop Museum base station, Honolulu, with the portable gravimeter.
- 1500 Shipboard gravity meter system on.
- 1732; Gravity tie #2 at pier 2C, Port of Honolulu with the portable gravimeter.
- 1910; Departed Pier 2C, Port of Honolulu, weather sunny and calm.

#### Day 004

- 0004; Large data error induced while tracking signals sent to the ABC system. Weather sunny and calm.

#### Day 005

- 0127 Deploy XBT #067 (T-04).
- 0335 Deploy 3.5kHz and 10kHz systems.
- 0350 Deploy GLORIA, amplifier malfunction.
- 0435 Deploy magnetometer.
- 0900 GLORIA system on, PPA repaired, begin data collection.

- 1935 Deploy two-channel streamer and airgun.
- 2043 SOL-001 (22°31.13'N, 159°08.32'W).
- 2127 Pressure loss on airgun. Gun pulled and hose replaced.
- 2200 Airgun restarted, seismic data collection resumed.  
Weather sunny and calm.

Day 006

- 0151 Deploy XBT #068 T-04  
Weather sunny and calm.

Day 007

- 0053 Deploy XBT #069 (T-04)  
Weather partly cloudy, seas moderate 1-2 m, winds 20 knots.

Day 008

- 0047 Deploy XBT #070 (T-07)  
Weather moderate to calm.  
Transmission of Telex 1 to USGS

Day 009

- 0152 Crossed International Dateline at 26° 02.72'N
- 0040 Deploy XBT #071 (T-04)
- 1235 EOL-001 (26° 28.90'N, 178° 30.10'E)
- 1310 SOL-002 (26° 28.90'N, 178° 30.10'E)
- 1520 EOL-002 (26° 48.60'N, 178° 17.50'E)
- 1531 SOL-003 (26° 48.60'N, 178° 17.50'E)
- 1945 Pulled 3.5 kHz fish in order to eliminate system noise

2007 Re-deployed 3.5-kHz fish; minor improvement in record. Weather: Seas moderate to rough. Winds 20-25 knots, seas 2-3 m.

#### Day 010

0154 Deploy XBT #072 (T-04)  
Weather: Winds 25 increasing to 35 knots, seas 3-5 m.

#### Day 011

1620 EOL-003 (24° 44.61'N, 174° 39.18'W). Continued deterioration of weather and shift of seas from north to east led to the decision to end line 003 and work toward the west.

1641 SOL-004 (24° 45.87'N, 174° 38.50'W)

1838 EOL-004 (25° 01.90'N, 174° 45.21'W)

1848 SOL-005 (25° 02.99'N, 174° 46.30'W)

2043 TCAG system off; air-gun change.

2145 TGAC system on.

Weather: winds 30-40 knots with gusts to 50 in the early morning, seas 5-6 m, improvement in mid-morning to winds of 20-25 knots, seas to 3 m.

Day 012 0045 Deploy XBT #073 (T-04)

Weather clear and calm.

#### Day 013

0042 Deploy XBT #074 (T-04).

1546 EOL-005 (27° 08.020'N, 178° 07.020'E).

1554 SOL-006 (27° 08.640'N, 178° 06.060'E)

1747 EOL-006 (27° 25.450'N, 178° 00.010'E).

1757 SOL-007 (27° 26.210'N, 178° 00.870'E).

1852 Slow speed (5 knots) to change 3.5 kHz fish; noisy records.

1918 3.5 kHz system on, marked improvement of 3.5 kHz records.

1922 Ship speed return to normal.

Weather partly cloudy with occasional showers.

Winds increased from 10 to 30 knots.

#### Day 014

2204 TCAG system on, but channel two inoperative.

#### Day 015

1857 TCAG system off, pulling streamer, ship speed 5 knots.

1918 Ship speed returned to normal, streamer pulled.

2015 EOL-007 (25° 15.00'N, 174° 35.70'W).

2059 SOL-008 (25° 15.00'N, 174° 35.70'W).

#### Day 016

0001 Decrease ship speed to 6 knots, redeploy repaired streamer.

0009 EOL-008 (24° 47.86'N, 174° 49.65'W).

0024 SOL-009 (24° 47.86'N, 174° 49.65'W).

0030 Ship speed returned to normal, streamer deployed.

0057 TCAG system on, streamer operation restored.

0158 Deploy XBT #075 (T-04).

Weather: winds 20-30 knots, seas to 2 m.

#### Day 017

2013 TCAG off, reposition streamer 50 meters closer to ship to investigate origin of clicking noise.

2017 TCAG system on.

2358 Deploy XBT #076 (T-04).

Day 018

1502 EOL-009 (22° 16.50'N, 166° 21.60'W).

1513 SOL-010 (22° 13.00'N, 166° 07.00'W).

1652 EOL-010 (22° 26.75'N, 166° 05.85'W).

1701 SOL-011 (22° 27.67'N, 166° 06.63'W).

2338 Deploy XBT #077 (T-07) Weather: winds 20 knots,  
seas to 2 m and improving.

Day 019

2333 Deploy XBT #078 (T-04)

Weather: winds 10 knots, seas to 2 m and worsening  
in the evening.

Day 020

1135 Masscomp stopped (problem).

1315 Masscomp restarted, resumed recording.

Day 021

0026 Deploy XBT #79 (T-04).

0424 EOL-011 (25° 02.99'N, 174° 46.30'W).

0430 SOL-012 (25° 02.99'N, 174° 46.30'W).

0801 EOL-012 (25° 16.17'N, 174° 37.92'W).

0816 SOL-013 (25° 16.17'N, 174° 37.92'W).

2252 TCAG system off, change air-gun.

Day 022

0022 TCAG system on.

0045 Deploy XBT #80 (T-04).

Day 023



- 2123 Deploy XBT #81 (T-04).
- 2025 TCAG system off, Masscomp stopped.
- 2054 TGAC system on, Masscomp restarted, resume recording.

#### Day 024

- 0023 Deploy XBT #82 (T-07).
- 0142 EOL-013 (22°39.60'N, 165°50.00'W).
- 0156 SOL-014 (22°39.60'N, 165°50.00'W).
- 0342 EOL-014 (22°50.20'N, 165°35.30'W).
- 0353 SOL-015 (22°50.20'N, 165°35.30'W).
- 1800 EOL-015 (23°27.08'N, 167°37.64'W), end data collection for F1-90-HW.
- 1806 Retrieve GLORIA, streamer, airgun, magnetometer, 3.5- & 10-kHz towfish.
- 1941 TRA-2 to Honolulu (23°27.320' N, -167°42.290'W).

#### Day 025

- 0029 Deploy XBT #83 (T-04).

#### Day 027

- 1800 Dock at Port of Honolulu, Hawaii.

### Equipment Summary

A description of the equipment used for shipboard data collection is presented below. Detailed compilation of shipboard data collection and performance of equipment is recorded in the DAFE data archive for F1-90-HW. Appendix I summarizes standard operational procedures

established during the 1986 surveys (Normark et al., 1987 and 1989). Appendix 2 is an abridged version of the DAFE data record for F1-90-HW.

### *Gravity Meter*

The gravity meter, a LaCoste and Romberg S-53, functioned continuously for the entire cruise. A land-sea gravity tie was established at pier 2C in Honolulu prior to departure by taking reference measurements at the Bishop Museum IGSN gravity base station, Honolulu, with LaCoste and Romberg model G portable gravity meter number 426. Another land-sea gravity tie was established following the cruise so that drift corrections could be applied to the data. Gravity measurements were recorded on magnetic tape and on a strip-chart recorder.

### *Magnetometer*

The magnetometer was deployed at JD 005/0435Z. The measurements were recorded on both a strip chart and magnetic tape along with the gravity data. There were no serious problems with the system. Some spikes on measured values occurred when seas were very rough, apparently caused by sensor pitching when the ship pitched, thereby yanking the tow cable. The magnetometer was recovered on JD026/1806Z.

### *Expendable Bathythermographs (XBT's)*

XBT probes typically were deployed once daily, beginning on JD 005, to measure the thickness of the ocean surface mixed layer and the thermocline temperature profile. Occasionally, XBT drops were canceled, or they failed due to excessive wind or ship motion. T-4 probes are capable of profiling to 460 m water depth, and T-7 XBT's can profile to 760 m. T-7 probes were deployed weekly whereas T-4 probes were used for the intervening 6 days. The system consists of an XBT launcher and receiver, a GOES satellite transmitter, and a micro-computer/controller for recording, data output, and data transmission. The system performed well. The probe was launched using a 1.5 m extension handle, off the port side of the vessel and 6 m forward of the stern. The following list is a record of the location of daily XBT drops.

Day	XBT type	Depth rating	XBT number	Latitude	Longitude
004	T-04	460 m	67	21 20.9'N	159 04.3'W
006	T-04	460 m	68	22 45.3'N	168 51.4'W
007	T-04	460 m	69	23 49.5'N	172 26.9'W
008	T-07	760m	70	24 55.0'N	176 06.9'W
009	T-04	460 m	71	26 00.0'N	179 50.2'W
010	T-04	460 m	72	26 20.4'N	179 54.0'E
012	T-04	460 m	73	25 18.8'N	175 39.6'E
012	T-04	460 m	74	26 25.1'N	179 25.7'W
016	T-04	460 m	75	24 43.9'N	174 36.4'W
017	T-04	460 m	76	22 50.1'N	168 13.6'W
018	T-07	760 m	77	22 44.9'N	167 04.0'W
019	T-04	460 m	78	23 48.0'N	170 34.6'W

021	T-07	460 m	79	24 52.4'N	174 10.2'W
022	T-04	460 m	80	24 44.9'N	172 51.8'W
023	T-04	460 m	81	22 50.3'N	166 25.8'W
024	T-07	760 m	82	22 43.0'N	166 01.0'W
025	T-04	460 m	83	23 10.7'N	166 45.3'W

### *3.5-kHz High-Resolution Profiling System*

The 3.5-kHz transducer tow fish was deployed on JD 005/0335Z. Problems with record quality began within the first few days of the cruise. On JD 013/1852Z the tow fish was changed and the tail section was found to be loose and damaged. Record quality after repair was excellent. The tow fish was recovered on JD 024/1806Z.

### *10-kHz Echo-Sounding System*

The 10-kHz echo-sounding tow fish was deployed on JD 005/0335Z. The system worked well, with down time only for routine maintenance. The tow fish was recovered on JD 024/1806Z.

### *Two-Channel Seismic-Reflection System*

The two-channel seismic reflection system employs a 2600 cm<sup>3</sup> (160 in<sup>3</sup>) air-gun sound source, and an 800 m weight-stabilized two-channel streamer. Two 50-m-long transducer sections are towed 500 to 600 m behind the air gun, which is fired every 10 seconds. Two-channel data is

recorded real-time on a MASSCOMP computer and displayed on a graphics monitor set to receive a one-channel, 2.3-second analog record. During the survey, two single-channel analog hard copy profiles were produced on Raytheon line scan recorders (LSR), one with 8-second sweep and the other with 6-second sweep. The memory function on the 6-second record was used to print at a constant orientation (west and north are on the left, east and south are on the right) At a speed of 8.5 knots, vertical exaggeration is about 4:1 on the 6-second record and 20:1 on the 8-second record.

The two-channel seismic reflection system had a number of problems during our survey. At JD 014/2204Z, channel one on the streamer ceased functioning. Several attempts were made to correct the malfunction, but without success. On JD 015/1857 the streamer was retrieved and found to be physically damaged in two places. The protective sleeve at the back end of the first stretch section had pulled apart, and the streamer was held together only by the conductive cables and one strength member. The missing signal problem was found in the tow cable of the streamer. These problems were corrected, and the streamer was redeployed at JD 016/0001Z. A hammering noise problem developed in the streamer cable during the last half of the cruise and apparently was related to rotation of the Farnella's propeller. A shipyard diver was hired to inspect the propeller section for foreign material. Final recovery was at 024/1806Z.

### *Navigation Systems*

Shipboard navigation (described in Normark et al., 1987) was monitored on the bridge for steering and recorded in the lab for archival.

A USGS in-house program operating on an IBM PC AT processed both Loran and GPS signals. Loran signals from a Northstar 7000 receiver were acquired to calculate direct range on Loran stations (referred to as RhoRho navigation). Global Positioning System (GPS) signals received on a Trimble 4000 receiver provided the most accurate fixes and were available almost 16 hours per day. RhoRho navigation was used to monitor the ship's track when GPS was unavailable.

### *GLORIA Long Range Side-scan Sonar System*

The GLORIA system was launched on JD 005/0350Z and a PPA amplifier malfunction occurred on system start-up. IOS GLORIA engineers corrected the problem by replacing the component, and the system was restarted at JD 005/0900Z. Thereafter, the system operated without problems for the duration of the survey. Logging of GLORIA data began almost immediately after deployment of the tow fish. To avoid spurious echo returns, signal transmission was suspended during course changes. The system operated continuously until the termination of the survey on JD 024/1806Z. Then, the GLORIA tow fish was recovered following the recovery of the magnetometer and seismic gear.

The deployment and operation of the GLORIA system is described in detail in IOS GLORIA logs. Technical descriptions of the GLORIA system are available in Somers et al. (1978) and Laughton (1981). A summary of the GLORIA pass record and the number of files is presented in Appendix 2. Note that one pass equals 6 hours.

### *GLORIA Shipboard Image Processing*

The techniques employed in shipboard processing are described in detail in Normark et al. (1987 and 1989). Special shading techniques, such as those used by Normark et al. (1989), were not applied. Following the photo printing of the GLORIA passes, the images were laid down over a properly scaled, corrected and smoothed navigation plot and then mosaicked.

## **RESULTS**

The following outline organizes the topics addressed:

### **1. Cretaceous seafloor and volcanic features**

- 1a. Murray Fracture Zone
- 1b. Seafloor spreading fabric
- 1c. Seamount distribution and characteristics
- 1d. Cretaceous ridges
- 1e. Lava flows

### **2. Sedimentation**

- 2a. Sediment in acoustic-reflection profiles
- 2b. Sediment in GLORIA images
- 2c. Seafloor channels
- 2d. Bedforms

### **3. Mass wasting features**

- 3a. Debris avalanches and small scale mass wasting features.

### **1. Cretaceous seafloor and volcanic features**

- 1a. Murray Fracture Zone (MFZ)

Three strongly displayed lineations and two weaker ones, both probably representing fault offset of the seafloor, were imaged in the survey and are interpreted to be part Murray Fracture Zone (Figure 3).



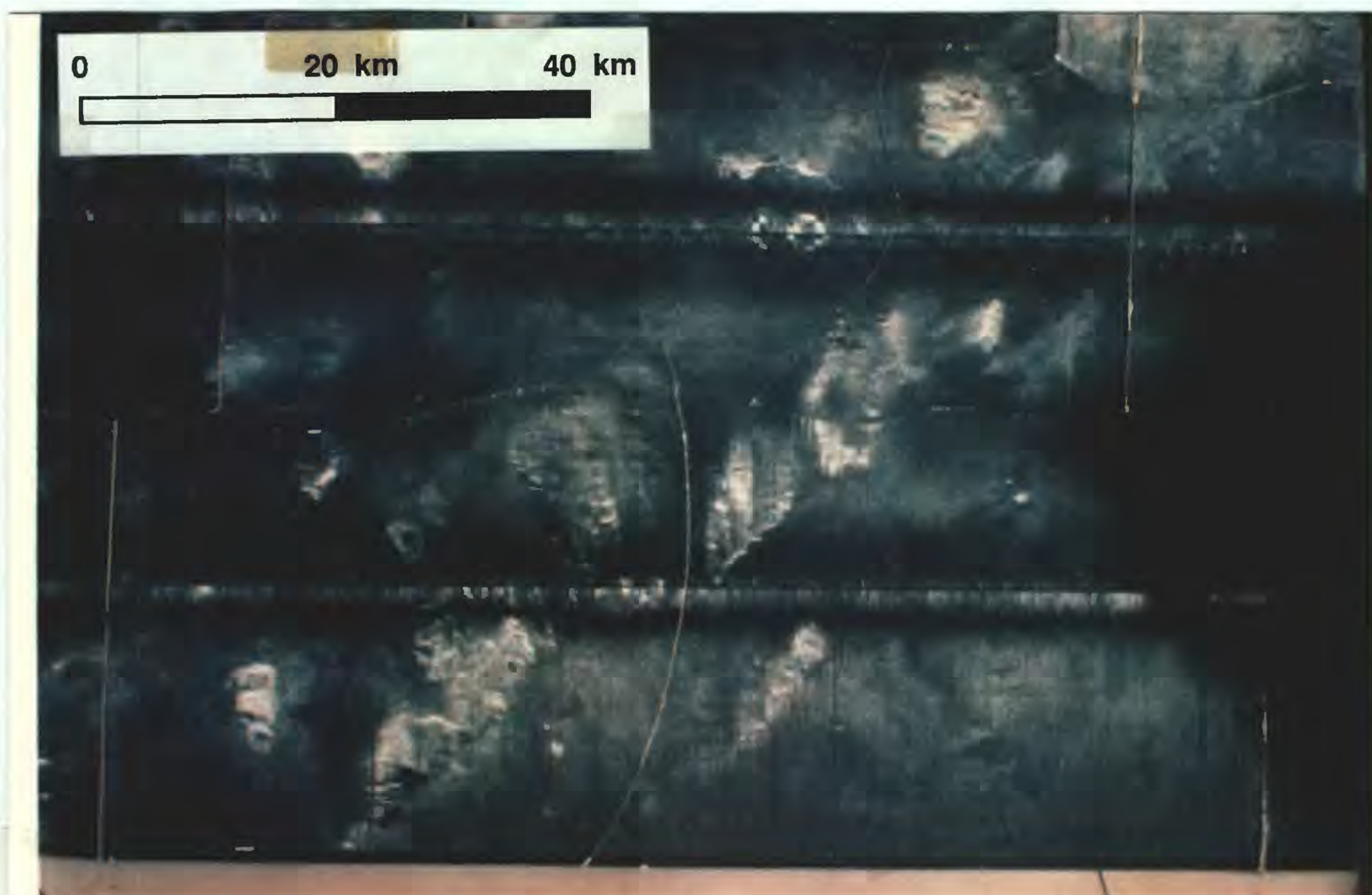


Figure 3. GLORIA sonograph of the Murray Fracture Zone (MFZ).



The lineations lie parallel to, but offset from, two additional lineations imaged to the south-east during F13-89-HW. The lineations lie between  $176^{\circ} 30'W$  and  $175^{\circ} 15'W$  and trend N65E. The three more strongly displayed lineations consist of en-echelon leaky faults. Flood basalts(?) (Volcanic ridges?) and occasional seamounts rise above the surrounding sediment along the fault trace. However, much of the survey area interpreted to be within the MFZ is sediment covered. The three lineations are spaced 8 to 9 km apart. The two more weakly expressed lineations, 37 and 75 km northeast of the stronger ones, are defined by the alignment of seamounts and volcanic ridges. For example, four seamounts aligned at N65E are centered at about  $176^{\circ} 'W$ ,  $24^{\circ} 55'N$ . Two seamounts of this group produce relatively low backscatter and apparently are draped with a relatively thick section (approximately 30 meters) of acoustically transparent sediment, whereas the other two produce relatively strong backscatter and are draped with only 20 meters of sediment on average. The Murray Fracture Zone within our study area therefore is thought to comprise at least five parallel faults spanning a total width of approximately 90 km. When combined with the adjacent and parallel offset features imaged in the previous survey, the Murray Fracture zone appears to be approximately 150 km wide and has a surface outcrop expression of at least seven faults.

A fault parallel to the MFZ occurs at  $179^{\circ} 30'W$ ,  $26^{\circ} 20'N$  oriented N65E. This fault truncates a prominent outcrop of oceanic basement rock to the south that clearly exhibits drag-folded spreading fabric, suggesting left-lateral motion along the fault (Figure 4). This block is interpreted to be dipping gently to the southeast, resulting in eventual burial of the seafloor spreading fabric.



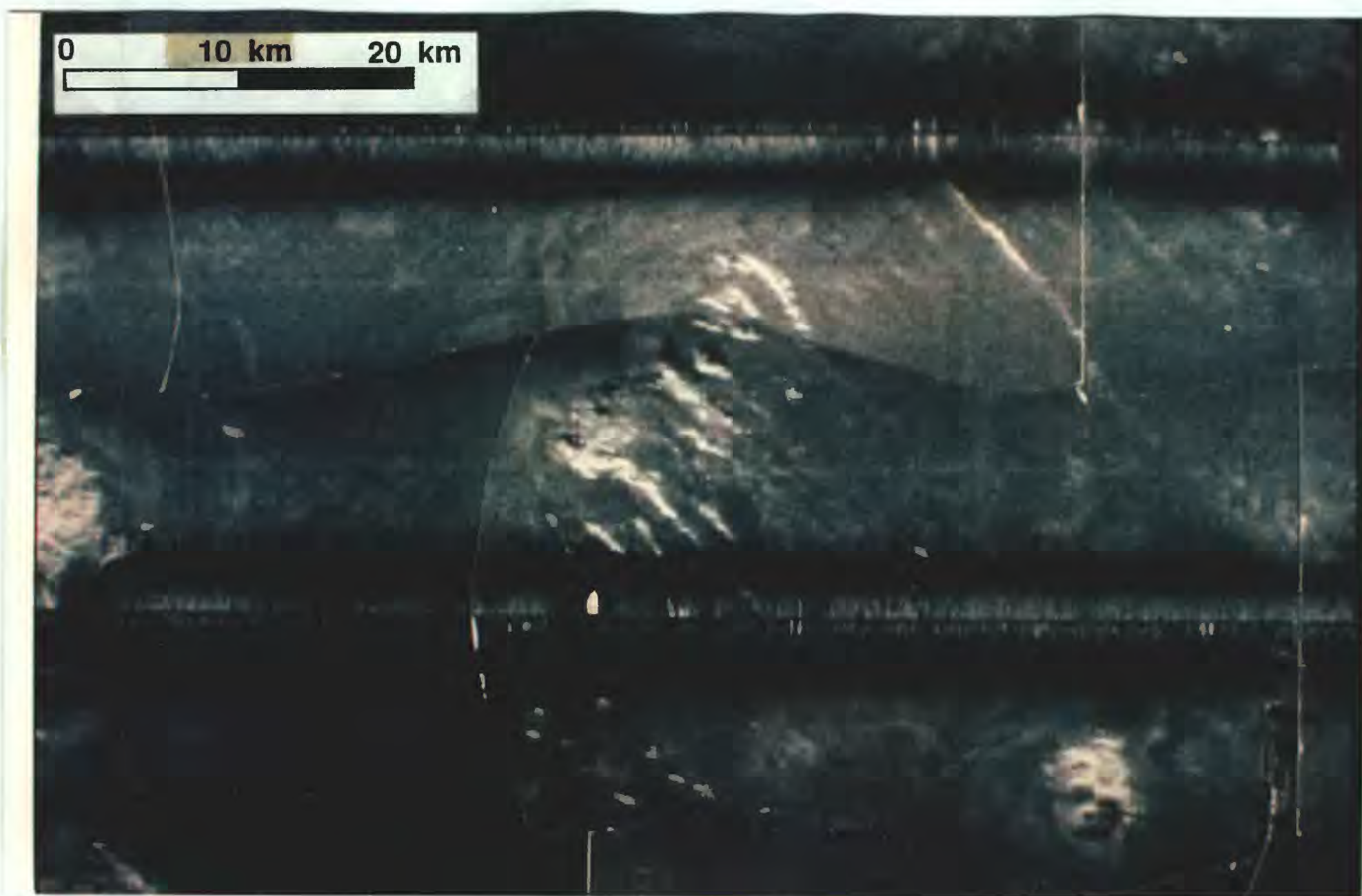


Figure 4. GLORIA sonograph of seafloor spreading fabric and left lateral strike-slip faulting parallel to the MFZ system.



### 1b. Seafloor spreading fabric

Seafloor spreading fabric can be seen clearly where original Cretaceous basement rock outcrops or is overlain by a relatively thin (<20 meter) veneer of acoustically transparent sediment. The most apparent expression of the horst and graben fabric is at the west end of the study area, between 178° 40'W and 178° 00'E (Figure 5). Horsts in this abyssal hills province strike uniformly N25W to N26W and are spaced 1.5 to 5 km apart. Individual horsts can be traced obliquely across the width of the survey area, approximately 160 kilometers. The spreading fabric was generated at the East Pacific Rise approximately 95-128 M.a.

The distinct alternating backscatter intensity across the spreading fabric between 178° 40'W and 178° 00'E may be caused by; (1) different sediment thickness over the ridges compared to the valleys, resulting in variations in backscatter from buried features (see below); (2) different sediment properties over the ridges compared to the valleys; and (3) topography of the ridge and valley fabric itself. In support of the first and second possibilities, the transparent layer that drapes much of the study area appears to thin over the graben and includes a hard layer with a strong acoustic signature. This reflective layer typically is not present above the horsts. In support of the third case, topographic expression of the spreading fabric is displayed in the reflection profiles. However, the variations in backscatter intensity do not change character with direction of insonification, which supports the first two possibilities and argues against the third. The abyssal hills region may have formed in response to upward



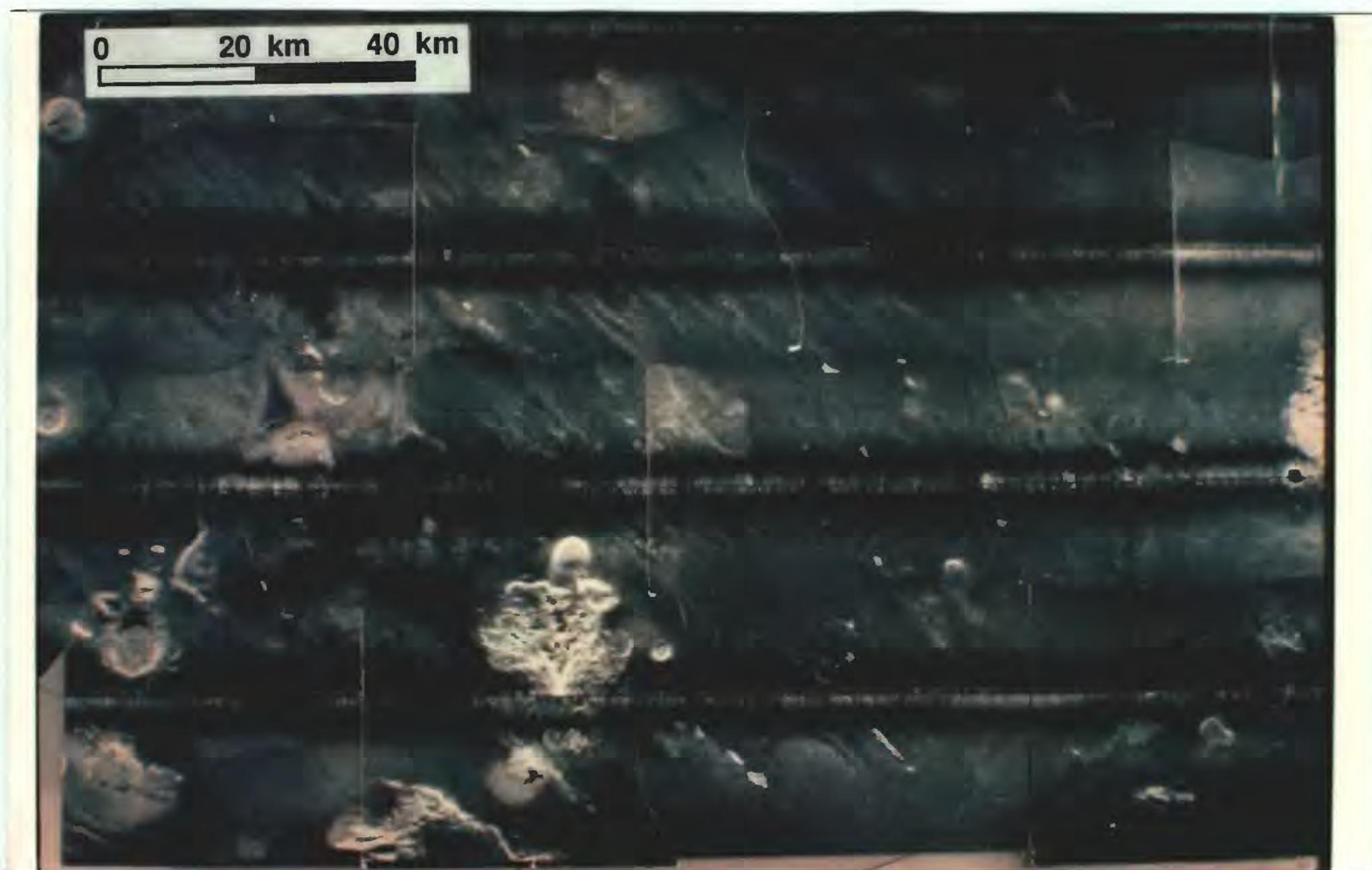


Figure 5. Seafloor spreading fabric across the western portion of the study area.

crustal flexure not present in other portions of the survey area, or it may be due to larger offset of the normal faults.

#### 1c. Seamount distribution and characteristics

Four seamount types are present within the survey region, although some seamounts possess characteristics attributable to more than one type. The four general types are:

- I) small (generally 3-10 km across) smooth-surfaced, circular, low-relief seamounts with or without summit craters.
- II) large (>10 km across) rough-surfaced, possibly degraded, non-circular seamounts.
- III) small (5-10 km across) rough-surfaced, possibly degraded, non-circular seamounts.
- IV) very small (less than 2 km across) rough-surfaced volcanic mounds or spatter cones.

The following tables list all seamounts classifiable as TYPE-I,-II, or -III. Seamounts are listed by longitude, with the seamount farthest west listed first, followed by seamounts to the east.

TYPE I: Small (less than 10 mi), round, low-relief seamounts					
Location	No	Diam. (mi.)	Flow Features	Summit Crater	Comments
178° 18'E 26° 57'N	1	2.7	No	No	

178° 32'E 26° 48'N	2	2.6	No	Yes	
178° 34'E 26° 30'N	3	3.0	No	Yes	Possibly degraded on west side
178° 43'E 27° 08'N	4	3.6	No	No	
179° 10'E 26° 27'N	5	2.8	No	Possible	North of degraded volcano
179° 15'E 26° 15'N	6	1.5	Possibly to north	Possible	
179° 41'W 26° 25'N	7	2.1	No	Yes	North of degraded volcano
177° 19'W 25° 49'N	8	1.2	North, possibly south	No	May have subsidiary volcano.
175° 55'W 25° 32'N	9	1.6	No	No	
175° 25'W 26° 40'N	10	1.2	?	No	
169° 36'W 22° 50'N	11	4.5	No	No	
169° 24'W 22° 48'N	12	4.0	Yes	Yes	Adjacent seamount to south may be type-1 volcano
169° 12'W 23° 06'N	13	4.2	No	Yes	
169° 00'W 22° 57'N	14	3.6	No	No	
168° 54'W 22° 42'N	15	1.2	Yes	Yes	
168° 48'W 22° 48'N	16	3.0	No	No	West side possibly degraded
168° 20'W 23° 00'N	17	3.9	No	No	
168° 00'W 22° 45'N	18	4.5	No	?	
167° 25'W 23° 05'N	19	3.0	No	Yes	
167° 10'W 22° 51'N	20	2.4	No	Yes	
167° 10'W 22° 45'N	21	3.0	No	Yes	
166° 26'W 22° 24'N	22	2.9	No	No	
166° 22'W 22° 10'N	23	2.1	No	No	
166° 16'W 26° 08'N	24	2.9	No	No	

166° 10'W 22° 25'N	25	3.8	No	No	
--------------------	----	-----	----	----	--

**TYPE II: Large, non-circular and rough-surfaced seamounts**

Location	No	Diam. (mi.)	Flow Features	Summit Crater	Comments
178° 45'E 26° 12'N	26	5-6	Possible	No	Difficult to interpret, at edge of mosaic
179° 45'W 26° 20'N	27	9.6	No	No	Very strong backscatter, rough surface
179° 06'W 26° 21'N	28	8.1	No	No	Very rough surface
177° 55'W 26° 23'N	29	12.0	Yes	?	
177° 20'W 25° 45'N	30	12.5	No	No	Very strong backscatter, rough surface
177° 09'W 25° 07'N	31	7.5	No	No	May be composite of smaller volcanoes, low backscatter intensity.
175° 40'W 24° 36'N	32	~15	No	No	
174° 10'W 24° 47'N	33	6.0	No	No	
174° 00'W 24° 35'N	34	6.0	No	No	Gullied
173° 58'W 24° 20'N	35	6.0	No	Yes	
173° 51'W 24° 38'N	36	10.0	No	No	
173° 47'W 24° 20'N	37	15.0	No	Yes	Prominent volcanic ridge to south
173° 45'W 24° 50'N	38	~15	No	Yes	May be source of lava flow(?) to the east.



173° 06'W 24° 20'N	39	8.0	No	No	
173° 00'W 24° 00'N	40	10x30	No	No	Highly degraded guyot with well developed amphitheatres and debris flows. Debris blocks up to 3 km wide
172° 45'W 24° 50'N	41	~40.0	No	No	Highly degraded guyot, well defined amphitheatres. Possible reef on summit. Large volcanic ridge on eastern flank.
168° 10'W 22° 24'N	42	15+	Yes	No	Ridge feature is composite of many volcanoes

3: Small, non-circular, rough-surfaced or degraded seamounts					
Location	No	Diam. (mi.)	Flow Features	Summit Crater	Comments
178° 18'E 26° 29'N	43	3.5	No	No	
178° 18'E 26° 33'N	44	1.2	No	No	
178° 30'E 26° 54'N	45	2.6	No	No	
178° 30'E 27° 00'N	46	3.0	No	No	
179° 03'E 26° 14'N	47	1.8	Strong halo	No	Seamount on horst of seafloor spreading fabric
179° 30'E 26° 24'N	48	3.3	No	No	Surrounded and topped by unusual cluster of very small volcanic mounds

179° 05'W 25° 57'N	49	3.0	Possible	No	Possible small debris flow below amphitheater.
178° 27'W 25° 00'N	50	up to 5.0	No	No	Field of at least 13 rough-surfaced seamounts
178° 24'W 25° 42'N	51		No	No	
178° 03'W 25° 48'N	52	1.0	No	No	
176° 00'W 24° 48'N	53	3.0	No	No	Elongated axis strikes N60E.
175° 30'W 24° 36'N	54	6.0	No	No	Associated with MFZ (group 58, 54)
175° 24'W 25° 00'N	55	1.9	No	No	Associated with MFZ (group 53, 55, 57)
175° 20'W 25° 17'N	56	4.5	Flow to South	No	Volcanic ridge axis strikes N20E
175° 12'W 25° 05'N	57	5.0	No	No	Associated with MFZ (group 53, 55, 57)
175° 00'W 24° 55'N	58	3.5	No	No	Associated with MFZ (group 58, 54)

A number of small, typically isolated volcanoes of round, low-relief (Type I) occur throughout the F1-90-HW study area. They have a peripheral, steep slope that appears on the GLORIA images as a narrow band of strong backscatter surrounding a relatively low-backscatter, relatively flat central area (Figure 6, seamount in top center). The topography is confirmed in acoustic profiles across these features. These volcanoes are similar in morphology to many of those studied on or adjacent to the East Pacific Rise (Fornari, 1984).

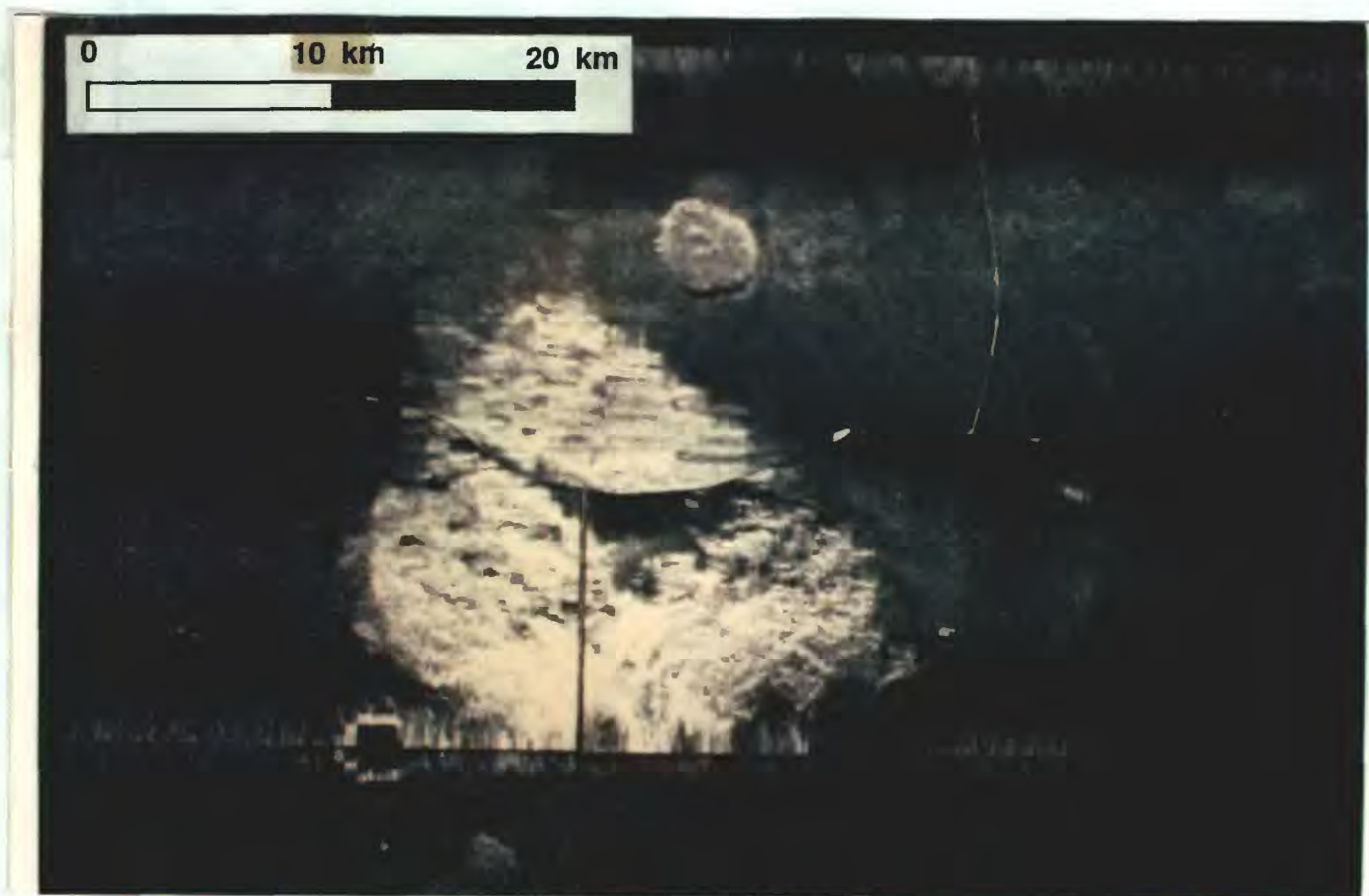


Figure 6. Type 1 (top center) and Type 2 (middle center) seamounts.



A conspicuous halo region surrounds many Type I volcanoes. The halo is irregular in shape and almost certainly is not a GLORIA processing artifact. Rather, the halos may represent volcanic material (lava flows, ejecta) shed from the seamount during its formation, or sediment deposited subsequently through mass-wasting.

Large, steep, and rough-surfaced seamounts of generally high backscatter intensity (Type II) occur in the study area. These volcanoes are highly mottled and irregular in shape on the GLORIA images, and they may be a cluster of volcanic mounds super-imposed upon one another during a dome building process (Figure 6, seamount in middle center). The Type-II Cretaceous (?) seamounts do not appear to be oriented along any lineaments or faults.

A group of large seamounts and guyots is located south of the main axis of the Hawaiian Island chain between  $173^{\circ}\text{W}$ ,  $24^{\circ}\text{N}$  and  $174^{\circ}\text{W}$ ,  $25^{\circ}\text{N}$  (Figure 7). They probably are Cretaceous in age, older than the adjacent Hawaiian islands. Horizon Guyot, a large, extensively studied Cretaceous tablemount 660 km to the southeast, rises approximately 3,500 m above the abyssal seafloor to within 1,400 m of the sea surface, similar to the guyots in our study area (Heezen et al., 1971). Characteristic of these seamounts are one or more flank ridges emanating from the main volcanic cone, similar to the Puna ridge at the southeast end of Hawaii (Holcomb et al. 1988). The ridges are extensively gullied, and several possess well developed amphitheaters, below which lie large debris avalanche fans. Individual blocks incorporated within the slide debris are as much as 3 km across, and some of the slide material may be collapsed coral reefs.



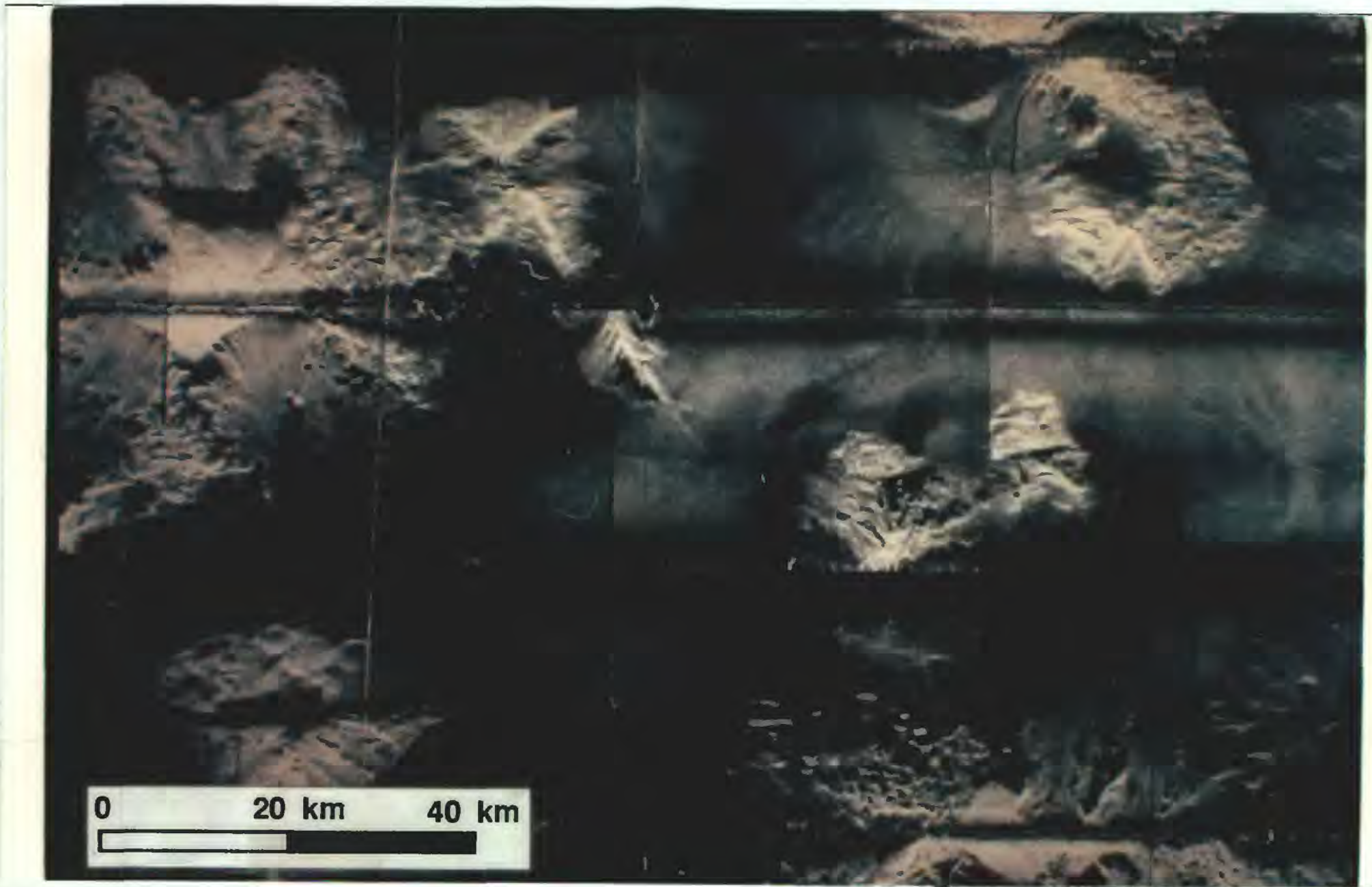


Figure 7. Guyots in the central portion of the study area.



As in our study area, debris flows that emanate from the summit sediment cap and bedrock flanks of Horizon Guyot are present in talus deposits and onto the adjacent abyssal seafloor, suggesting that mass wasting is an important process that controls the morphology of these seamounts (Schwab et al., 1988, Kayen et al., 1990). Although the group of large seamounts may be Cretaceous in age, their close proximity to the Hawaiian Ridge probably exposed them to higher levels of environmental loading compared to seamounts elsewhere. These environmental stresses include earthquake loading, crustal subsidence and arching due to loading by the ridge, and partial volcanic overprinting by the propagating Hawaiian hot spot. This may have caused more extensive mass wasting relative to other, isolated large abyssal seamounts.

Discontinuous, strongly backscattering edges occur along the perimeter of the summit cap of the two largest guyots. They are most clearly visible on the southerly edge of the guyots' rim. Possibly, these are drowned reefs.

Type III seamounts are rough-surfaced and largely non-circular (Figure 8). They probably are Cretaceous in age and formed on the seafloor soon after its creation at the East Pacific Rise some 95-128 Ma.

Very small (less than 1.5 km across) seamounts and volcanic mounds are classified as Type IV. This group was not cataloged in the tables above. Type IV seamounts are spread over most of the study area and uncommonly occur in clusters. These seamounts probably are also Cretaceous in age.



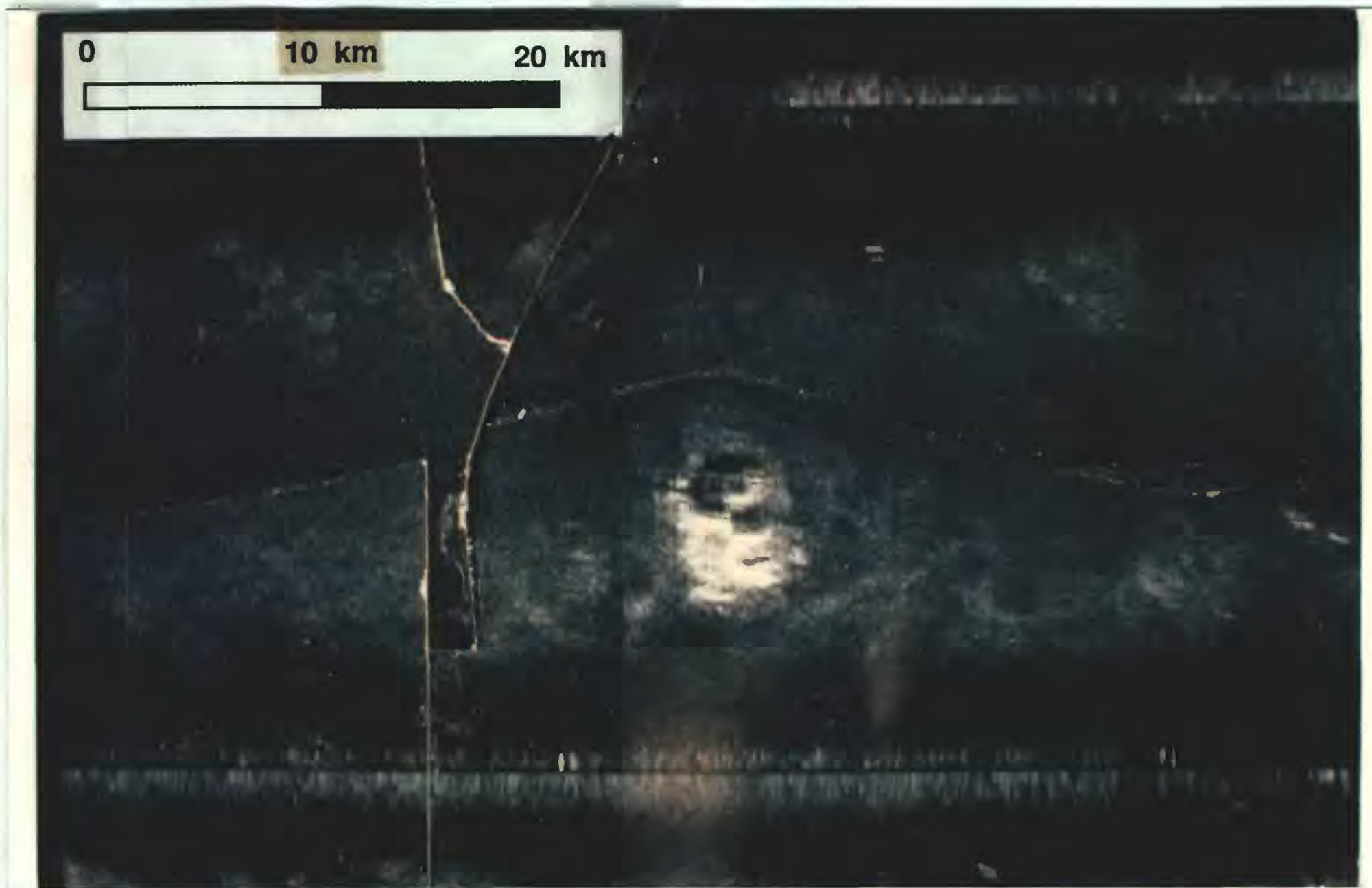


Figure 8. Type 3 seamount characterized by its relatively small size and bright, rough backscatter intensity.



#### 1d. Cretaceous ridges

Necker Ridge at the east end of the survey area appears to have formed from massive eruptions along three parallel leaky transform faults that trend N48E. The crests of the volcanic ridges are spaced at 45 km and separated by two intervening sediment-filled basins (Figure 9). The most southern and massive ridge is Necker Ridge, which is, on average, 25 km wide and rises 3,200 m above the abyssal seafloor to within 1,600 m of the sea-surface. More detailed discussions of Necker Ridge were made by Pickthorn et al. (in press) and Torresan et al. (in press).

#### 1e. Lava flows

A long sheet flow was imaged near a large Type II volcano at 173° 45'W, 26° 20'N. It apparently flowed downslope to the south for at least 65 km. However, the flow is nowhere more than 10 km across. The sheet flow is interpreted to have had low viscosity (Figure 10). Acoustic profiles across the flow indicate that it lies within a shallow topographic depression and has an opaque, and characteristically weak, "mushy" reflector, similar to lava flows imaged off Oahu (Torresan, et al., 1989), and Hawaii (Normark et al., 1987). The flow covers at least 820 km<sup>2</sup> and surrounds three isolated kapuki. The lava flow possibly extends another 20 miles toward the south but is obscured by a thicker sediment drape.





Figure 9. Necker ridge and an adjacent ridge to the northwest. The intervening region is a sediment filled basin.



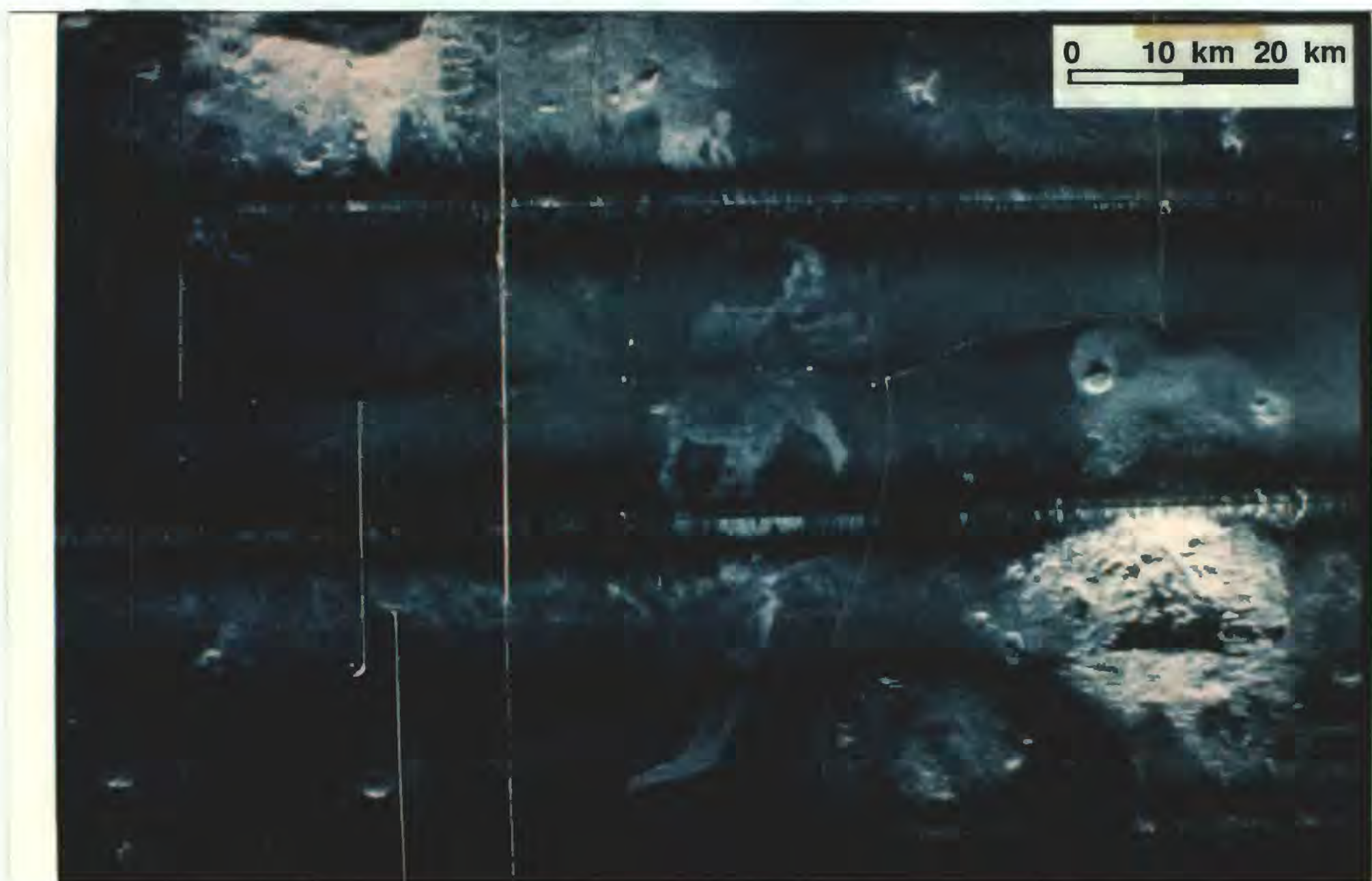


Figure 10. Lava flow following low topography between seamounts. \



## 2. Sedimentation

### 2a. Sediment in acoustic-reflection profiles

The air-gun profiles show a sequence of nearly horizontal, parallel reflectors that reach a thickness of more than 0.6 sec (two-way travel time) over oceanic basement. The reflectors have a basin fill pattern; that is, reflectors truncate against, rather than drape, the irregular basement surface. The reflector sequence is absent in places where the oceanic crust reaches the seafloor. The sequence has been interpreted as turbidite and hemipelagic basin fill (Torresan et al. in press).

The 3.5-kHz profiles show a transparent drape, most likely pelagic or hemipelagic sediment, covering the seafloor throughout most of the area. This layer is up to 0.050 sec thick but most commonly is between 0.010 and 0.030 sec thick (Figure 11). Its upper surface (the seafloor) is a sharp, strong reflector. Internally, the layer may be either totally transparent, or it may contain one or a few continuous to discontinuous, sharp to prolonged reflectors, especially near seamounts and volcanic ridges. These internal reflectors probably are volcanoclastic sediment beds formed by material shed off the adjacent rock masses. The transparent layer drapes most topographic features such as basement ridges and seamounts, but it is undetectable over some of the seamounts that have strong backscatter in the GLORIA images. For example, the guyots and seamounts in the vicinity of 24° 40' N, 173° 40' W typically are not draped by the transparent layer. Instead, their surface has an opaque, prolonged reflector that suggests bare volcanic rock or volcanoclastic sediment.



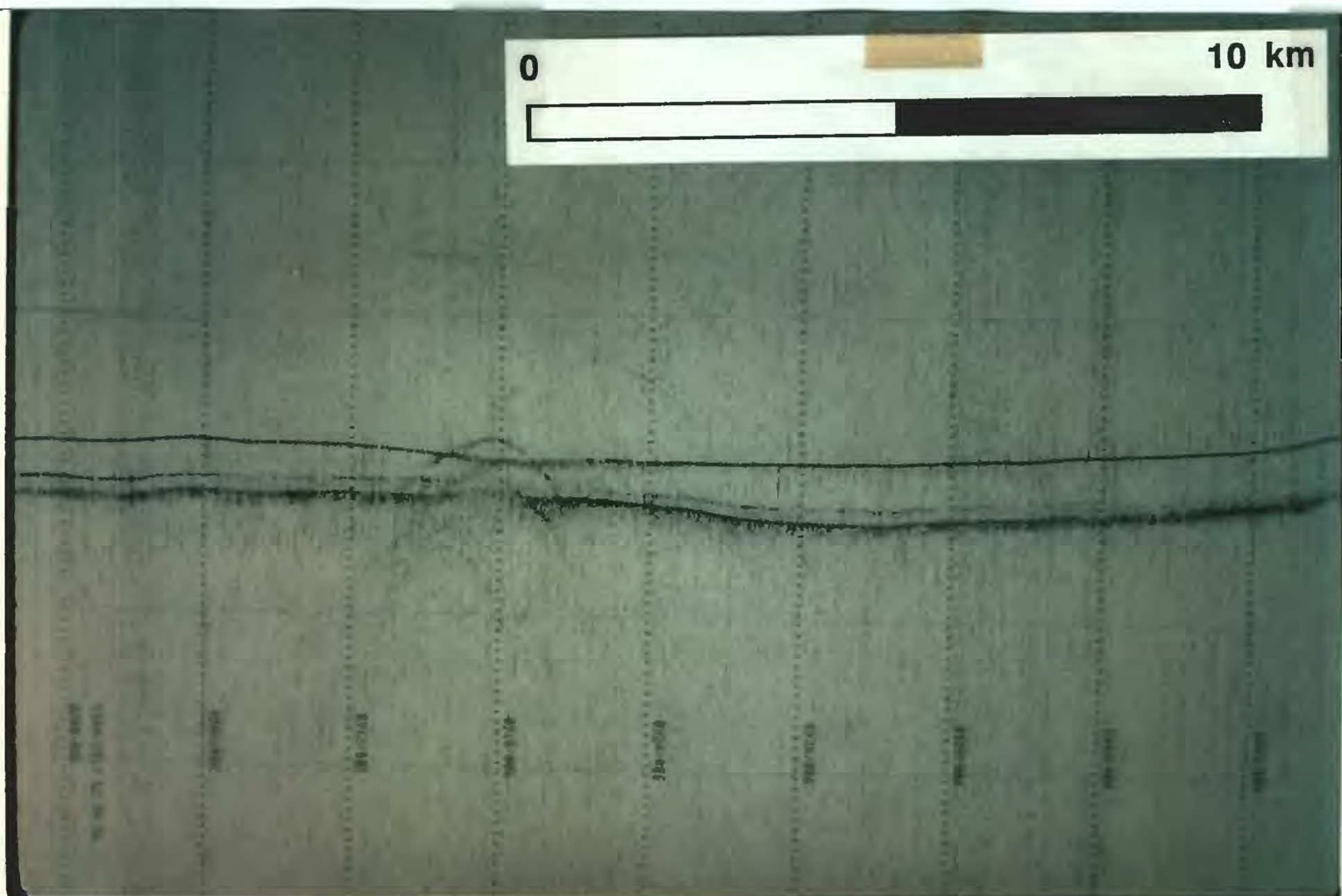


Figure 11. 3.5 kHz record of the transparent sediment layer.



Most commonly, a prolonged to opaque reflector is present at the base of the transparent layer. In some places, hyperbolic reflections occur along the basal reflector. Uncommonly, stratified sediment is visible beneath the transparent layer.

## 2b. Sediment in GLORIA images

Sediment-covered seafloor has a range of backscatter intensities on GLORIA images, depending on the thickness of the transparent layer, the presence of internal reflectors within the transparent layer, and the nature of material or topography beneath the transparent layer. GLORIA's acoustic energy may penetrate up to 0.025 ms through the transparent layer and therefore in many places the images could display the backscatter characteristics of buried features. To wit, the images are dark along tracklines where the transparent layer is greater than about 0.025 sec thick, especially if no internal reflectors are present and the underlying surface is smooth. At the other extreme, the backscatter is strong surrounding the guyots where a dark, prolonged reflector in the 3.5-kHz profiles suggests volcanoclastic sediment at the seafloor. Farther away along some tracklines, the backscatter decreases gradationally to dark shades, and the 3.5 kHz profile shows a thickening transparent layer that is absent close to the seamount or guyot. Elsewhere, in the abyssal hills province at the western end of the area, the Cretaceous seafloor grain is manifest as a pattern of elongate, alternating light and dark backscatter contrasts that do not vary with direction of insonification, suggesting that the contrast is not due to the topography associated with the hills. The 3.5 kHz profiles



indicate the presence of a strong reflector within the transparent layer, only in the valleys between the hills, and this reflector likely explains the backscatter contrasts. Other examples of backscatter variation in areas covered by the transparent drape exist throughout the area. Evidently, GLORIA acoustic energy can penetrate up to a few tens of meters of pelagic sediment to return backscattered energy from buried features.

#### 2c. Seafloor channels

A sea-channel/sediment-dispersal system was identified at 172° 35'W, 23° 55'N. At least two tributary channels coalesce and appear to funnel sediment toward the southeast, to a region insonified during F13-89-HW. Here, other tributaries transport sediment from seamounts south and west of the channel to a depocenter located at approximately 172° 00'W, 23° 20'N. A topographic low across the channel measured at three transit line crossings (1 during F1-90-HW, 2 during F13-89-HW) does not exceed 8 meters and is, in places, barely perceptible below the background variations in topography.

#### 2d. Bedforms

An area of possible current-generated bedforms exists in the vicinity of the guyots, centered at about 172° 10'W 24° 40'N (Figure 12). The GLORIA images have a sinuous, alternating light and dark pattern, with a repetition length of about 1.5 km. The 3.5 kHz profiles show a relatively complicated stratigraphy and structure, with a discontinuous transparent layer, truncated reflectors, and some wavy reflectors. Possibly, regional



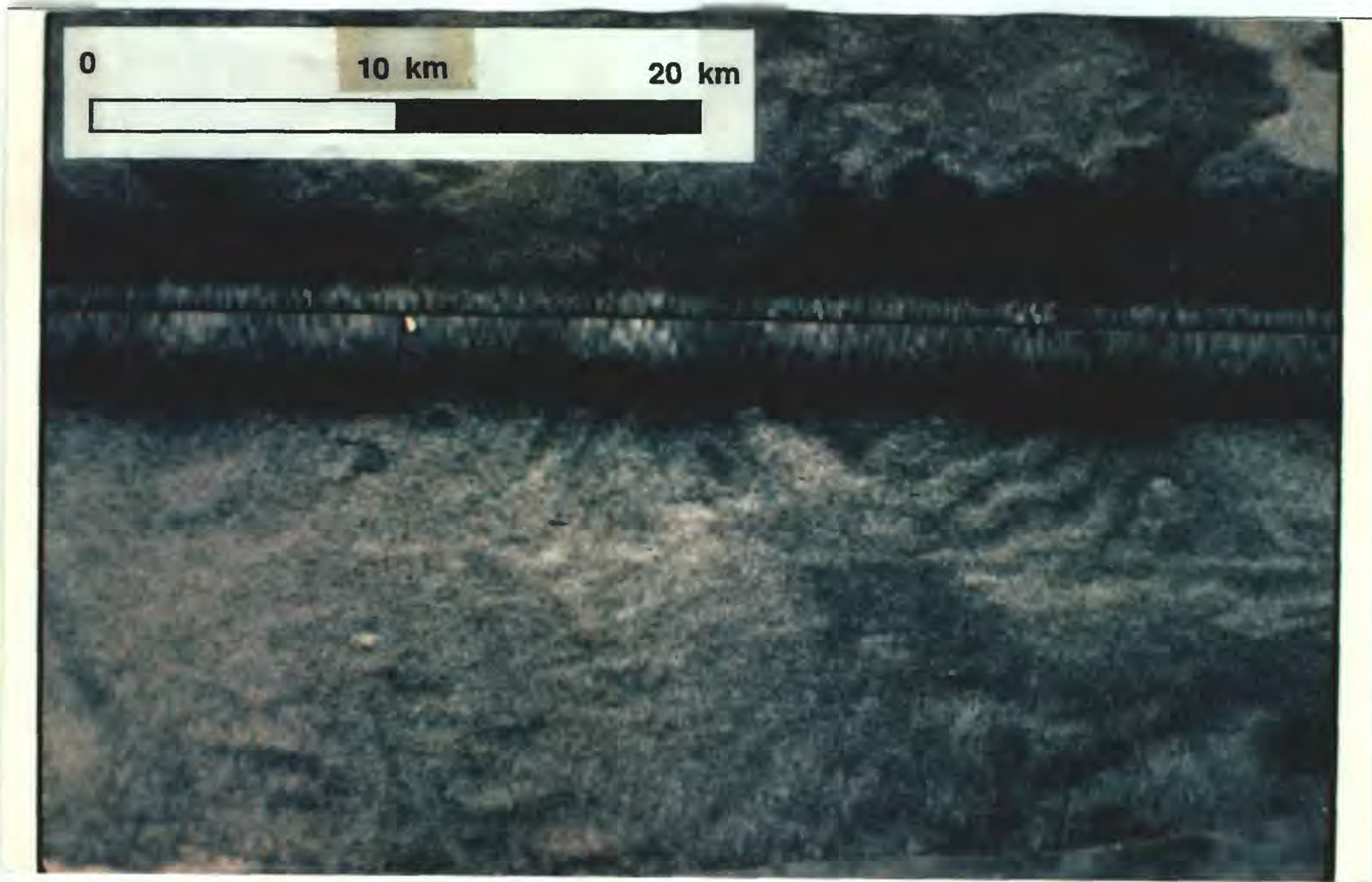


Figure 12. Bedform field in the central portion of the study area.



currents around the guyots are intensified to erosional, bedform-producing levels.

### **3. Mass wasting features**

#### **3a. Debris avalanches and small scale mass wasting features.**

A giant debris avalanche, informally named the Neva slide, is similar to features imaged with GLORIA off the Hawaiian Islands (Moore et al., 1989). This slide was imaged at 174° 45'W, 25° 25'N and may have flowed southwest from the slopes of Lisianski Island and Neva shoal, approximately 90 km upslope from the toe of the slide. The toe of the slide is characterized by large isolated blocks incorporated in an apparently finer matrix of debris (Figure 13). Individual slide blocks are as much as 1 km long. The broad fan of isolated blocks at the toe, as well as the apparently large distance between source area and distal deposits suggest that the slide was a fast moving and highly mobilized debris avalanche. The following survey, F2-90-HW, will image the upper portion of the slide and the source area which will better define the slide morphology and run-out length.

A number of large, rough-surfaced seamounts appear to have gullies and debris chutes, and several have well developed amphitheatres and debris avalanche deposits. These features suggest that mass wasting is an important component that affects the morphologic development of seamounts. As stated in section 1c, the Cretaceous seamount cluster near the Hawaiian islands may have been exposed to higher levels of



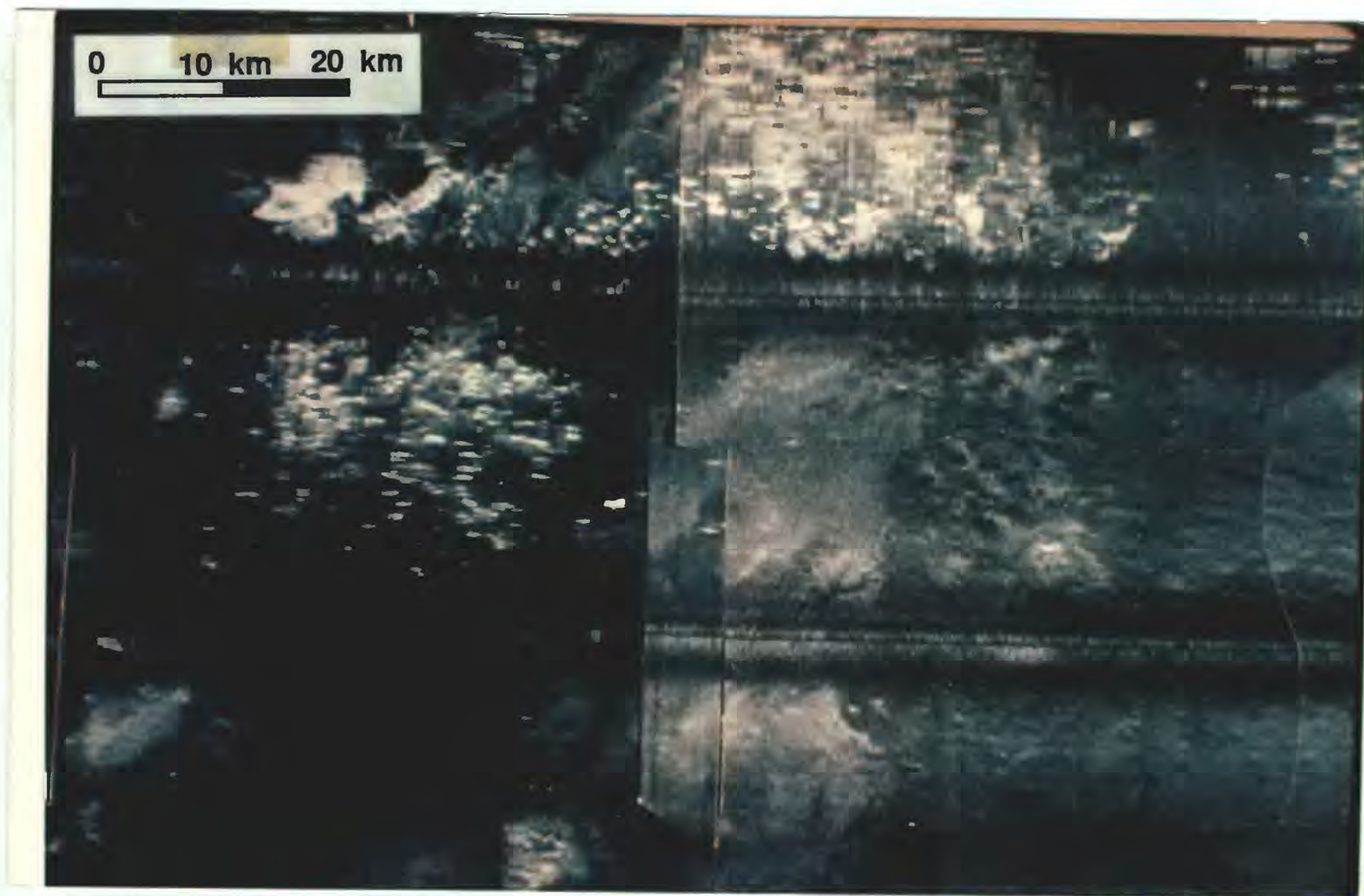


Figure 13. Massive debris flow deposit insonified by GLORIA in the central portion of the study area.

environmental loading than seamounts in other regions of the abyssal seafloor. This cluster appears to be extensively eroded in GLORIA images, particularly the two guyots.

## ACKNOWLEDGEMENTS

We wish to thank Captain Ronald Holliday and crew of the M/V Farnella, and the scientific and technical staffs of the USGS and IOS, whose help and professionalism contributed to the success of the survey. We also wish to thank Dave Drake for reviewing the manuscript.

## REFERENCES

- Atwater, T. and Severinghaus, J., 1989, Tectonic maps of the northeast Pacific, *in*, Winterer, E.L., Hussong, D.M., and Decker, R.W., eds., The Eastern Pacific Ocean and Hawaii: Boulder, Colorado, Geological Society of America, The Geology of North America, Vol. N.
- Chase, T.E., Menard, H.W., and Mammerick, J., 1972, Bathymetry of the North Pacific, Scripps Institute of Oceanography and Institute of Marine Resources, chart no. 8.
- Clague, D.A., Moore, J.G., Torresan, M.E., Holcomb, R.T., and Lipman, P.W., 1988, Shipboard report for Hawaii Gloria ground-truth cruise

F2-88-HW, 25 February - 9 March, 1988: U.S. Geological Survey  
Open-File Report 88-292, 54 p.

Fornari, D.J., and Ryan, W.B.F., The evolution of craters and calderas on young seamounts: Insights from Sea MARC I and Sea Beam sonar surveys of a small seamount group near the axis of the East Pacific Rise at  $\sim 10^{\circ}\text{N.}$ , Jour. Geophys. Res., Vol. 89, No. B13, pp. 11,069-11,083.

Holcomb, R.T., Moore, J.T., Lipman, P.W., Belderson, R.H., 1988, Voluminous submarine lava flows from Hawaiian volcanoes, Geology, v. 16, p. 400-404.

Kayen, R.E., Schwab, W.C., Lee, H.J., Torresan, M.E., Hein, J.R., Quinterno, P.J., and Levin, L.A., 1989, Morphology of sea-floor landslides on Horizon Guyot: application of steady-state geotechnical analysis, Deep-Sea Research. Vol. 36, No. 12, pp. 1817-1838.

Moore, J.G., Clague, D.A., Holcomb, R.T., Lipman, P.W., Normark, W.R., and Torresan, M.E., 1989, Prodigious Submarine Landslides on the Hawaiian Ridge, Jour. Geophys. Res., Vol. 94, No. B12, pp. 17,465-17,484.

Normark, W.R., Lipman, P.W., Wilson, J.B., Jacobs, C.L., Johnson, D.P., and Gutmacher, C.E., 1987 Preliminary Cruise Report, Hawaiian GLORIA Leg 2, F6-86-HW, November 1986, USGS Open-File Report 87-298.

Normark, W.R., Holcomb, R.T., Searle, R.C., Somers, M.L., and  
Gutmacher, C.E., 1989 Cruise Report, Hawaiian GLORIA Legs 3  
and 4, F3-88-HW and F4-88-HW, USGS Open-File Report 89-213

Pickthorn, L.B., Drake, D. et al., in press, F13-89-HW Cruise Report,  
USGS Open-File Report

Schwab, W.C., Lee, H.J., Kayen, R.E., Quinterno, P.J., and Tate, G.B.,  
1988, Erosion and Slope Instability on Horizon Guyot, Mid-Pacific  
Mountains, Geo-Marine Letters, No. 8, pp. 1-10.

Torresan et al., in press, F12-89-HW Cruise report, USGS Open-File  
Report

Torresan, M.E, Shor, A.N., Wilson, J.B., Campbell, J., 1989, Cruise  
Report, Hawaiian GLORIA Leg 5, F5-88-HW, USGS Open-File  
Report No. 89-198.

## **APPENDIX I**

### **EQUIPMENT SETTINGS AND COMMENTS**

#### **3.5 kHz SYSTEM**

LSR Recorder

Mode - Continuous  
PAPER - 100 lpi  
SWEEP - 1 sec  
PROGRAM - As required

	GAIN - Mid
	CONTRAST - Mid
	THRESHOLD - Min
PTR Transceiver	GAIN - 6
	POWER - max
	PULSE WIDTH - Not used
IOS Correlator	OUTPUT LEVEL - 4-5
	ATTENUATOR - 11.5

Fish Depth Compensation 7 m.

### *10 KHz SYSTEM*

MUFAX Recorder	ATTENUATOR - -6 to -18
	TIME MARKS - 6 min.
	PULSE LENGTH - 2.8 to 5
	FISH DEPTH - 2x5 m
	GATING SELECTOR - 6
	FATHOMS/METERS - Meters
	TRIGGER (Left/Center) -as required for scale changes
	TVG - not used
	GATING - Use to "see" bottom through outgoing pulse.

### *MAGNETOMETER/GRADIOMETER*

Soltec Recorder	CHART SPEED - 40 cm/hr
	Full scale at 100 gamma range

### *GRAVIMETER*

Soltec Recorder	CHART SPEED - 10 cm/hr
-----------------	------------------------

### *SEISMIC REFLECTION SYSTEM*

LSR Recorder	DISPLAY - Normal
	STYLUS SCAN - 2 sec
	PAPER - 120 lpi
	MEMORY SWEEP - 6 sec
	FILTER - out
	POLARITY - +
	GAIN 10 to 2 O'clock
	CONTRAST -30 to -40
	THRESHOLD - 2
Krohn - Hite Filter	20-120 Hz
Masscomp	GAIN SETTING: Pre-amp 0
	Post-amp 6 to 18
DMD Delay Box	As required for DWD

..... Appendix 2.  
DAFE data archive .....

**DAFE CRUISE DATA INDEX**

**FCR**

**F 1 90 HW**

**SHIP: Farnella**

**CHIEF SCIENTIST: Hampton/Kayen**

**TIME DATUM: GREENWICH MEAN TIME**

**LISTING GENERATED: 27-Mar-1990**

.....

RECORDING MEDIA      DATE AND TIME      STATUS      ACTIVITY      LINE STA- REEL      LATITUDE      LONGITUDE      R SAMP U  
 TION SAMPLE DEC DEG    DEC DEG    C DPTH N

.....

DATA CATEGORY = HYDROLOGICAL

.....

.....SYSTEM = TEMPERATURE/SALINITY/CONDUCTANCE GAUGES

.....DATA OR EQUIPMENT CODE = EXP. BATHY THERMOGRAPH

D-DEPLOYMENT OF SCIENTIFIC GEAR 90 005 0127	SAMPLE DEPLOY XBT #67 (T-04)	:TRA1;	:0067	20.82987	-155.25188	Y:4500;m
D-DEPLOYMENT OF SCIENTIFIC GEAR 90 006 0151	SAMPLE DEPLOY XBT #68 (T-04)	:0001;	:0068	22.75750	-168.86040	Y:4650;m
D-DEPLOYMENT OF SCIENTIFIC GEAR 90 007 0053	SAMPLE DEPLOY XBT #69 (T-04)	:0001;	:0069	23.82595	-172.44870	Y:4685;m
D-DEPLOYMENT OF SCIENTIFIC GEAR 90 008 0047	SAMPLE DEPLOY XBT #70 (T-07)	:0001;	:0070	24.90995	-176.11790	Y:5180;m
D-DEPLOYMENT OF SCIENTIFIC GEAR 90 009 0040	SAMPLE DEPLOY XBT #71 (T-04)	:0001;	:0071	25.99930	-179.83980	Y:5515;m
D-DEPLOYMENT OF SCIENTIFIC GEAR 90 010 0154	SAMPLE DEPLOY XBT #72 (T-04)	:0003;	:0072	26.33950	179.89620	Y:5495;m
D-DEPLOYMENT OF SCIENTIFIC GEAR 90 012 0045	SAMPLE DEPLOY XBT #73 (T-04)	:0005;	:0073	25.31305	-175.66260	Y:5080;m
D-DEPLOYMENT OF SCIENTIFIC GEAR 90 013 0042	SAMPLE DEPLOY XBT #74 (T-04)	:0005;	:0074	26.41970	-179.43120	Y:5360;m
D-DEPLOYMENT OF SCIENTIFIC GEAR 90 016 0158	SAMPLE DEPLOY XBT #75 (T-04)	:0009;	:0075	24.73120	-174.60270	Y:5000;m
D-DEPLOYMENT OF SCIENTIFIC GEAR 90 017 2358	SAMPLE DEPLOY XBT #76 (T-04)	:0009;	:0076	22.83280	-168.21860	Y:4762;m
D-DEPLOYMENT OF SCIENTIFIC GEAR 90 018 2338	SAMPLE DEPLOY XBT #77 (T-07)	:0011;	:0077	22.75000	-167.06650	Y:4770;m
D-DEPLOYMENT OF SCIENTIFIC GEAR 90 019 2333	SAMPLE DEPLOY XBT #78 (T-04)	:0011;	:0078	23.80080	-170.57890	Y:4636;m
D-DEPLOYMENT OF SCIENTIFIC GEAR 90 021 0026	SAMPLE DEPLOY XBT #79 (T-04)	:0011;	:0079	24.87390	-174.17140	Y:4918;m
D-DEPLOYMENT OF SCIENTIFIC GEAR 90 022 0045	SAMPLE DEPLOY XBT #80 (T-04)	:0013;	:0080	24.74930	-172.86350	Y:2540;m
D-DEPLOYMENT OF SCIENTIFIC GEAR 90 023 2123	SAMPLE DEPLOY XBT #81 (T-04)	:0013;	:0081	22.83950	-166.43395	Y:4658;m
D-DEPLOYMENT OF SCIENTIFIC GEAR 90 024 0023	SAMPLE DEPLOY XBT #82 (T-07)	:0013;	:0082	22.71730	-166.01291	Y:4650;m
D-DEPLOYMENT OF SCIENTIFIC GEAR 90 025 0029	SAMPLE DEPLOY XBT #83 (T-04)	:TRAN;	:0083			Y:4700;m

W-INVENTORY OF SCIENTIFIC GEAR 90 027 0415

EXP. BATHY THERMOGRAPH ; ;

; ;

.....

DATA CATEGORY = VESSEL DATA

.....

\*\*\*\*\*SYSTEM - NAVIGATION

\*\*\*\*\*DATA OR EQUIPMENT CODE - INTEGRATED NAV

C-FLOPPY DISK OR PUNCH CARDS	90 003 1811	START	START OF DISK #01	;PORT;	;0001 15.46733 -115.28308 ; ;
C-FLOPPY DISK OR PUNCH CARDS	90 009 1908	END	END OF DISK #01	;0003;	;0001 26.63840 178.87920 ; ;
C-FLOPPY DISK OR PUNCH CARDS	90 009 1909	START	START OF DISK #02	;0003;	;0002 26.63765 178.88190 ; ;
C-FLOPPY DISK OR PUNCH CARDS	90 014 2116	END	END OF DISK #02	;0007;	;0002 26.32670 -178.17630 ; ;
C-FLOPPY DISK OR PUNCH CARDS	90 014 2118	START	START OF DISK #03	;0007;	;0003 26.32540 -178.17160 ; ;
C-FLOPPY DISK OR PUNCH CARDS	90 015 2122	END	END OF DISK #03	;0008;	;0003 25.19340 -174.66290 ; ;
C-FLOPPY DISK OR PUNCH CARDS	90 015 2128	START	START OF DISK #04	;0008;	;0004 25.18010 -174.67000 ; ;
C-FLOPPY DISK OR PUNCH CARDS	90 021 1710	END	END OF DISK #04	;0013;	;0004 25.06070 -173.92210 ; ;
C-FLOPPY DISK OR PUNCH CARDS	90 021 1711	START	START OF DISK #05	;0013;	;0005 25.06005 -173.91970 ; ;
C-FLOPPY DISK OR PUNCH CARDS	90 023 1309	END	END OF DISK #05	;0013;	;0005 23.19350 -167.61885 ; ;
C-FLOPPY DISK OR PUNCH CARDS	90 023 1405	START	START OF DISK #06	;0013;	;0006 23.15440 -167.48530 ; ;
C-FLOPPY DISK OR PUNCH CARDS	90 025 0750	END	END OF DISK #06	;TRAN;	;0006 ; ;
C-FLOPPY DISK OR PUNCH CARDS	90 025 0800	START	START OF DISK #07	;TRAN;	;0007 ; ;
C-FLOPPY DISK OR PUNCH CARDS	90 026 2300	END	END OF DISK #07	;TRAN;	;0007 ; ;

G-PAPER PRINTER LISTING	90 003 1811	START	START OF ROLL #01	;PORT;	;0001 15.46733 -115.28308 ; ;
G-PAPER PRINTER LISTING	90 026 2300	END	END OF ROLL #01	;TRAN;	;0001 ; ;



RECORDING MEDIA	DATE AND TIME	STATUS	ROLL ACTIVITY	LINE STA- REEL	LATITUDE	LONGITUDE	R SAMP	U
TION SAMPLE DEG DEG DEC DEG C DPTH N								
*****DATA OR EQUIPMENT CODE = LORAN C								
W-INVENTORY OF SCIENTIFIC GEAR	90 027 0415		LORAN C					
*****DATA OR EQUIPMENT CODE = GPS SATELLITE								
W-INVENTORY OF SCIENTIFIC GEAR	90 027 0415		GPS SATELLITE					
*****DATA OR EQUIPMENT CODE = CRUISE								
K-SHIP MOVEMENTS	90 003 1908	START	LV HONOLULU-START F190HW;TRAN;		15.63027	-116.49749		
K-SHIP MOVEMENTS	90 027 0400	END	END OF CRUISE/END OF F1-;TRAN;			0-;HW;		
*****DATA OR EQUIPMENT CODE = LORAN C RHO-RHO								
W-INVENTORY OF SCIENTIFIC GEAR	90 027 0415		LORAN C RHO RHO					
*****DATA OR EQUIPMENT CODE = TRACKLINE								
K-SHIP MOVEMENTS	90 005 2043	START	START OF LINE #01		22.51855	-168.06080		
K-SHIP MOVEMENTS	90 009 1235	END	END OF LINE #01		26.48195	178.50120		
K-SHIP MOVEMENTS	90 009 1310	START	START OF LINE #02		26.53910	178.43810		
K-SHIP MOVEMENTS	90 009 1520	END	END OF LINE #02		26.79470	178.26750		
K-SHIP MOVEMENTS	90 009 1531	START	START OF LINE #03		26.80705	178.28340		
K-SHIP MOVEMENTS	90 011 1625	END	END OF LINE #03		24.75030	-174.65780		
K-SHIP MOVEMENTS	90 011 1641	START	START OF LINE #04		24.77240	-174.65020		
K-SHIP MOVEMENTS	90 011 1838	END	END OF LINE #04		25.02690	-174.75190		
K-SHIP MOVEMENTS	90 011 1848	START	START OF LINE #05		25.05090	-174.77010		
K-SHIP MOVEMENTS	90 013 1546	END	END OF LINE #05		27.13230	178.11720		
K-SHIP MOVEMENTS	90 013 1554	START	START OF LINE #06		27.14560	178.10240		

K-SHIP MOVEMENTS	90 013 1747	END	END OF LINE #06	:0006;	27.42365	178.00230	;
K-SHIP MOVEMENTS	90 013 1757	START	START OF LINE #07	:0007;	27.43515	178.01500	;
K-SHIP MOVEMENTS	90 015 2051	END	END OF LINE #07	:0007;	25.26420	-174.63950	;
K-SHIP MOVEMENTS	90 015 2059	START	START OF LINE #08	:0008;	25.24530	-174.63820	;
K-SHIP MOVEMENTS	90 016 0009	END	END OF LINE #08	:0008;	24.82015	-174.84590	;
K-SHIP MOVEMENTS	90 016 0024	START	START OF LINE #09	:0009;	24.80030	-174.83350	;
K-SHIP MOVEMENTS	90 018 1502	END	END OF LINE #09	:0009;	22.20570	-166.12520	;
K-SHIP MOVEMENTS	90 018 1513	START	START OF LINE #10	:0010;	22.21855	-166.10971	;
K-SHIP MOVEMENTS	90 018 1653	END	END OF LINE #10	:0010;	22.44650	-166.09770	;
K-SHIP MOVEMENTS	90 018 1701	START	START OF LINE #11	:0011;	22.46105	-166.11186	;
K-SHIP MOVEMENTS	90 021 0424	END	END OF LINE #11	:0011;	25.05180	-174.77600	;
K-SHIP MOVEMENTS	90 021 0430	START	START OF LINE #12	:0012;	25.05980	-174.78830	;
K-SHIP MOVEMENTS	90 021 0801	END	END OF LINE #12	:0012;	25.39995	-175.17620	;
K-SHIP MOVEMENTS	90 021 0816	START	START OF LINE #13	:0013;	25.41690	-175.16050	;
K-SHIP MOVEMENTS	90 024 0142	END	END OF LINE #13	:0013;	22.65960	-165.83150	;
K-SHIP MOVEMENTS	90 024 0156	START	START OF LINE #14	:0014;	22.66340	-165.79800	;
K-SHIP MOVEMENTS	90 024 0342	END	END OF LINE #14	:0014;	22.81010	-165.56960	;
K-SHIP MOVEMENTS	90 024 0353	START	START OF LINE #15	:0015;	22.83005	-165.57036	;
K-SHIP MOVEMENTS	90 024 1800	END	END OF LINE #15	:0015;	23.45130	-167.62700	;
K-SHIP MOVEMENTS	90 024 1941	START	START TRAN TO HONOLULU	:TRAN;			;
K-SHIP MOVEMENTS	90 027 0400	END	END TRAN HONO PIER34	:TRAN;			;

RECORDING MEDIA      DATE AND TIME      STATUS      ACTIVITY      LINE STA- REEL      LATITUDE      LONGITUDE      R SAMP U  
TION SAMPLE DEC DEG      DEC DEG      C DPTH N

.....  
DATA CATEGORY = GEOPHYSICAL  
.....

\*\*\*\*\*SYSTEM = BATHYMETRY

\*\*\*\*\*DATA OR EQUIPMENT CODE = 10 KHZ BATHYMETRY

A-ANALOG PAPER ROLLS	90 005 0346	START OF ROLL #01	TRA1;	;0001	21.22721	-158.21330	;
A-ANALOG PAPER ROLLS	90 006 2000	END OF ROLL #01	;0001;	;0001	23.59420	-171.66420	;
A-ANALOG PAPER ROLLS	90 006 2001	START OF ROLL #02	;0001;	;0002	23.59505	-171.66660	;
A-ANALOG PAPER ROLLS	90 009 0825	END OF ROLL #02	;0001;	;0002	26.31265	179.08550	;
A-ANALOG PAPER ROLLS	90 009 0826	START OF ROLL #03	;0001;	;0003	26.31330	179.08330	;
A-ANALOG PAPER ROLLS	90 011 1842	END OF ROLL #03	;0004;	;0003	25.04030	-174.75870	;
A-ANALOG PAPER ROLLS	90 011 1844	START OF ROLL #04	;0005;	;0004	25.04440	-174.76170	;
A-ANALOG PAPER ROLLS	90 011 2112	END OF ROLL #04	;0005;	;0004	25.13970	-175.14400	;
A-ANALOG PAPER ROLLS	90 011 2115	START OF ROLL #05	;0005;	;0005	25.14165	-175.15160	;
A-ANALOG PAPER ROLLS	90 014 0624	END OF ROLL #05	;0007;	;0005	26.91890	179.79330	;
A-ANALOG PAPER ROLLS	90 014 0627	START OF ROLL #06	;0007;	;0006	26.91865	179.80030	;
A-ANALOG PAPER ROLLS	90 016 1824	END OF ROLL #06	;0009;	;0006	24.02410	-172.21260	;
A-ANALOG PAPER ROLLS	90 016 1828	START OF ROLL #07	;0009;	;0007	24.02150	-172.20360	;
A-ANALOG PAPER ROLLS	90 019 0624	END OF ROLL #07	;0011;	;0007	23.04910	-168.06300	;
A-ANALOG PAPER ROLLS	90 019 0627	START OF ROLL #08	;0011;	;0008	23.05120	-168.07000	;
A-ANALOG PAPER ROLLS	90 021 1825	END OF ROLL #08	;0013;	;0008	25.00670	-173.73990	;
A-ANALOG PAPER ROLLS	90 021 1829	START OF ROLL #09	;0013;	;0009	25.00355	-173.73040	;
A-ANALOG PAPER ROLLS	90 024 0648	END OF ROLL #09	;0015;	;0009	22.96280	-166.00500	;
A-ANALOG PAPER ROLLS	90 024 0650	START OF ROLL #10	;0015;	;0010	22.96430	-166.00980	;
A-ANALOG PAPER ROLLS	90 024 1806	END OF ROLL #10	;0015;	;0010	23.45460	-167.64000	;

W-INVENTORY OF SCIENTIFIC GEAR 90 027 0415      10 KHZ BATHYMETRY      ;      ;      ;

X-OPERATION OF SCIENTIFIC GEAR 90 005 0346      ON      SYS ON: BA10 DEPLYD      TRA1;      ;0001      21.22721      -158.21330      ;

X-OPERATION OF SCIENTIFIC GEAR 90 024 1806 OFF SYS OFF: END DATA COLL ;0015; ;0010 23.45460 -167.64000 ; ;

\*\*\*\*\*DATA OR EQUIPMENT CODE = 3.5KH BATHYMETRY

A-ANALOG PAPER ROLLS	90 005 0351	START	START OF ROLL #01	;TRA1;	;0001 21.24150 -158.31983 ;
A-ANALOG PAPER ROLLS	90 006 1957	END	END OF ROLL #01	;0001;	;0001 23.59165 -171.65690 ;
A-ANALOG PAPER ROLLS	90 006 1959	START	START OF ROLL #02	;0001;	;0002 23.59335 -171.66180 ;
A-ANALOG PAPER ROLLS	90 007 2009	END	END OF ROLL #02	;0001;	;0002 24.69775 -175.41630 ;
A-ANALOG PAPER ROLLS	90 007 2011	START	START OF ROLL #03	;0001;	;0003 24.69910 -175.42140 ;
A-ANALOG PAPER ROLLS	90 008 2020	END	END OF ROLL #03	;0001;	;0003 25.81080 -179.20500 ;
A-ANALOG PAPER ROLLS	90 008 2022	START	START OF ROLL #04	;0001;	;0004 25.81240 -179.21020 ;
A-ANALOG PAPER ROLLS	90 009 1235	END	END OF ROLL #04	;0001;	;0004 26.48195 178.50120 ;
A-ANALOG PAPER ROLLS	90 009 1240	START	START OF ROLL #05	;0002;	;0005 26.48620 178.48900 ;
A-ANALOG PAPER ROLLS	90 010 0509	END	END OF ROLL #05	;0003;	;0005 26.20310 -179.63730 ;
A-ANALOG PAPER ROLLS	90 010 0513	START	START OF ROLL #06	;0003;	;0006 26.20025 -179.62750 ;
A-ANALOG PAPER ROLLS	90 010 2008	END	END OF ROLL #06	;0003;	;0006 25.55900 -177.44710 ;
A-ANALOG PAPER ROLLS	90 010 2010	START	START OF ROLL #07	;0003;	;0007 25.55750 -177.44230 ;
A-ANALOG PAPER ROLLS	90 011 1836	END	END OF ROLL #07	;0004;	;0007 25.02690 -174.75190 ;
A-ANALOG PAPER ROLLS	90 011 1842	START	START OF ROLL #08	;0005;	;0008 25.04030 -174.75870 ;
A-ANALOG PAPER ROLLS	90 012 2007	END	END OF ROLL #08	;0005;	;0008 26.19945 -178.67580 ;
A-ANALOG PAPER ROLLS	90 012 2008	START	START OF ROLL #09	;0005;	;0009 26.20020 -178.67860 ;

RECORDING MEDIA	DATE AND TIME	STATUS	ROLL ACTIVITY	LINE STA- REEL	LATITUDE	LONGITUDE	R SAMP U
				TION SAMPLE DEC DEG	DEC DEG	C DPTH N	
-ANALOG PAPER ROLLS	90 013 0546	END	END OF ROLL #09	:0005;	:0009	26.64980	179.78140 ; ;
-ANALOG PAPER ROLLS	90 013 0551	START	START OF ROLL #10	:0005;	:0010	26.65370	179.76740 ; ;
A-ANALOG PAPER ROLLS	90 013 1748	END	END OF ROLL #10	:0006;	:0010	27.42580	178.00230 ; ;
A-ANALOG PAPER ROLLS	90 013 1800	START	START OF ROLL #11	:0007;	:0011	27.43480	178.02160 ; ;
A-ANALOG PAPER ROLLS	90 014 2007	END	END OF ROLL #11	:0007;	:0011	26.38085	-178.34740 ; ;
A-ANALOG PAPER ROLLS	90 014 2009	START	START OF ROLL #12	:0007;	:0012	26.37940	-178.34250 ; ;
A-ANALOG PAPER ROLLS	90 016 0009	END	END OF ROLL #12	:0008;	:0012	24.82015	-174.84590 ; ;
A-ANALOG PAPER ROLLS	90 016 0018	START	START OF ROLL #13	:0009;	:0013	24.80550	-174.84330 ; ;
A-ANALOG PAPER ROLLS	90 016 2010	END	END OF ROLL #13	:0009;	:0013	23.95270	-171.98170 ; ;
A-ANALOG PAPER ROLLS	90 016 2012	START	START OF ROLL #14	:0009;	:0014	23.95100	-171.97730 ; ;
A-ANALOG PAPER ROLLS	90 017 2011	END	END OF ROLL #14	:0009;	:0014	22.98945	-168.73890 ; ;
A-ANALOG PAPER ROLLS	90 017 2036	START	START OF ROLL #15	:0009;	:0015	22.97150	-168.68250 ; ;
A-ANALOG PAPER ROLLS	90 018 1655	END	END OF ROLL #15	:0010;	:0015	22.45120	-166.09990 ; ;
A-ANALOG PAPER ROLLS	90 018 1658	START	START OF ROLL #16	:0011;	:0016	22.45740	-166.10520 ; ;
A-ANALOG PAPER ROLLS	90 019 2006	END	END OF ROLL #16	:0011;	:0016	23.64700	-170.07170 ; ;
A-ANALOG PAPER ROLLS	90 019 2009	START	START OF ROLL #17	:0011;	:0017	23.64915	-170.07930 ; ;
A-ANALOG PAPER ROLLS	90 021 0425	END	END OF ROLL #17	:0011;	:0017	25.05295	-174.77830 ; ;
A-ANALOG PAPER ROLLS	90 021 0427	START	START OF ROLL #18	:0012;	:0018	25.05545	-174.78250 ; ;
A-ANALOG PAPER ROLLS	90 021 2010	END	END OF ROLL #18	:0013;	:0018	24.92540	-173.47890 ; ;
A-ANALOG PAPER ROLLS	90 021 2021	START	START OF ROLL #19	:0013;	:0019	24.91750	-173.45340 ; ;
A-ANALOG PAPER ROLLS	90 022 2006	END	END OF ROLL #19	:0013;	:0019	23.90960	-170.05510 ; ;
A-ANALOG PAPER ROLLS	90 022 2008	START	START OF ROLL #20	:0013;	:0020	23.90800	-170.05040 ; ;
A-ANALOG PAPER ROLLS	90 023 2010	END	END OF ROLL #20	:0013;	:0020	22.89330	-166.60660 ; ;
A-ANALOG PAPER ROLLS	90 023 2012	START	START OF ROLL #21	:0013;	:0021	22.89170	-166.60190 ; ;
A-ANALOG PAPER ROLLS	90 024 0142	END	END OF ROLL #21	:0013;	:0021	22.65960	-165.83150 ; ;
A-ANALOG PAPER ROLLS	90 024 0144	START	START OF ROLL #22	:0014;	:0022	22.65850	-165.82670 ; ;
A-ANALOG PAPER ROLLS	90 024 1806	END	END OF ROLL #22	:0015;	:0022	23.45460	-167.64000 ; ;
W-INVENTORY OF SCIENTIFIC GEAR	90 027 0415		3.5 KHZ BATHYMETRY	; ; ;			; ; ;
X-OPERATION OF SCIENTIFIC GEAR	90 005 0351	ON	SYS ON: BA35 DEPLYD	;TRA1;	:0001	21.24150	-158.31983 ; ;
X-OPERATION OF SCIENTIFIC GEAR	90 009 1945	OFF	SYS OFF: PULL 3.5 FISH	:0003;	:0005	26.60520	178.97520 ; ;

X-OPERATION OF SCIENTIFIC GEAR	90 009 2007	ON	SYS ON: FISH DEPLD	:0003;	:0005 26.58895	179.01650 ;
X-OPERATION OF SCIENTIFIC GEAR	90 013 1854	OFF	SYS OFF:CHG FISH	:0007;	:0011 27.39920	178.15960 ;
X-OPERATION OF SCIENTIFIC GEAR	90 013 1918	ON	SYS ON:FISH CHGD	:0007;	:0011 27.38660	178.20320 ;
X-OPERATION OF SCIENTIFIC GEAR	90 017 0716	OFF	SYS OFF: CLEAN RECRDR	:0009;	:0014 23.52210	-170.52530 ;
X-OPERATION OF SCIENTIFIC GEAR	90 017 0717	ON	SYS ON: RECRDR CLEANED	:0009;	:0014 23.52140	-170.52310 ;
X-OPERATION OF SCIENTIFIC GEAR	90 017 0722	OFF	SYS OFF: CLEAN RECRDR	:0009;	:0014 23.51790	-170.51190 ;
X-OPERATION OF SCIENTIFIC GEAR	90 017 0723	ON	SYS ON: RECDR CLEANED	:0009;	:0014 23.51725	-170.50980 ;
X-OPERATION OF SCIENTIFIC GEAR	90 019 0437	OFF	SYS OFF: RCDR REPAIRS	:0011;	:0016 22.97205	-167.80440 ;
X-OPERATION OF SCIENTIFIC GEAR	90 019 0503	ON	SYS ON: RCDR RESTORED	:0011;	:0016 22.99165	-167.86850 ;
X-OPERATION OF SCIENTIFIC GEAR	90 024 1808	OFF	SYS OFF: END DATA COLL	:0015;	:0022 23.45460	-167.64000 ;

\*\*\*\*\*SYSTEM = SHIPBOARD GRAVITY

\*\*\*\*\*DATA OR EQUIPMENT CODE = GRAVITY + MAGNET

M-DIGITAL MAGNETIC TAPES	90 003 1840	START	START OF TAPE #01	:PORT;	:0001 15.55023	-115.90093 ;
M-DIGITAL MAGNETIC TAPES	90 005 1731	END	END OF TAPE #01	:TRA1;	:0001 22.46425	-167.57040 ;
M-DIGITAL MAGNETIC TAPES	90 005 1733	START	START OF TAPE #02	:TRA1;	:0002 22.46485	-167.57600 ;
M-DIGITAL MAGNETIC TAPES	90 007 1305	END	END OF TAPE #02	:0001;	:0002 24.39190	-174.36070 ;
M-DIGITAL MAGNETIC TAPES	90 007 1307	START	START OF TAPE #03	:0001;	:0003 24.39350	-174.36580 ;
M-DIGITAL MAGNETIC TAPES	90 009 1320	END	END OF TAPE #03	:0002;	:0003 26.55920	178.42430 ;

RECORDING MEDIA	DATE AND TIME	STATUS	ROLL ACTIVITY	LINE STA-REEL	LATITUDE	LONGITUDE	R SAMP U
			TION SAMPLE	DEC DEG	DEC DEG	C DPTH N	
M-DIGITAL MAGNETIC TAPES	90 009 1322		START	START OF TAPE #04	-GRVM ;0002;	;0004 26.56320	178.42180 ; ;
M-DIGITAL MAGNETIC TAPES	90 011 1412		END	END OF TAPE #04	;0003;	;0004 24.83190	-174.94550 ; ;
M-DIGITAL MAGNETIC TAPES	90 011 1414		START	START OF TAPE #05	;0003;	;0005 24.83070	-174.94110 ; ;
M-DIGITAL MAGNETIC TAPES	90 013 1413		END	END OF TAPE #05	;0005;	;0005 27.06030	178.37420 ; ;
M-DIGITAL MAGNETIC TAPES	90 013 1415		START	START OF TAPE #06	;0005;	;0006 27.06185	178.36860 ; ;
M-DIGITAL MAGNETIC TAPES	90 015 1436		END	END OF TAPE #06	;0007;	;0006 25.55550	-175.58970 ; ;
M-DIGITAL MAGNETIC TAPES	90 015 1438		START	START OF TAPE #07	;0007;	;0007 25.55400	-175.58450 ; ;
M-DIGITAL MAGNETIC TAPES	90 017 1412		END	END OF TAPE #07	;0009;	;0007 23.24370	-169.59300 ; ;
M-DIGITAL MAGNETIC TAPES	90 017 1414		START	START OF TAPE #08	;0009;	;0008 23.24230	-169.58830 ; ;
M-DIGITAL MAGNETIC TAPES	90 019 0447		END	END OF TAPE #08	;0011;	;0008 22.97975	-167.82890 ; ;
M-DIGITAL MAGNETIC TAPES	90 019 0449		START	START OF TAPE #09	;0011;	;0009 22.98125	-167.83390 ; ;
M-DIGITAL MAGNETIC TAPES	90 021 0206		END	END OF TAPE #09	;0011;	;0009 24.94850	-174.42420 ; ;
M-DIGITAL MAGNETIC TAPES	90 021 0208		START	START OF TAPE #10	;0011;	;0010 24.95000	-174.42940 ; ;
M-DIGITAL MAGNETIC TAPES	90 023 0153		END	END OF TAPE #10	;0013;	;0010 23.67935	-169.24980 ; ;
M-DIGITAL MAGNETIC TAPES	90 023 0155		START	START OF TAPE #11	;0013;	;0011 23.67800	-169.24510 ; ;
M-DIGITAL MAGNETIC TAPES	90 024 1948		END	END OF TAPE #11	;TRAN;	;0011	; ;
M-DIGITAL MAGNETIC TAPES	90 024 1950		START	START OF TAPE #12	;TRAN;	;0012	; ;
M-DIGITAL MAGNETIC TAPES	90 025 0750		END	EOT #12: LAB POWER LOSS	;TRAN;	;0012	; ;
M-DIGITAL MAGNETIC TAPES	90 025 0803		START	START OF TAPE #13	;TRAN;	;0013	; ;
M-DIGITAL MAGNETIC TAPES	90 026 2300		END	END OF TAPE #13	;TRAN;	;0013	; ;
*****DATA OR EQUIPMENT CODE = GRAV, MAG, BATHYMETRY, AND NAVIGATION							
M-DIGITAL MAGNETIC TAPES	90 005 1000		START	SOT ABC/NAV,DEPTH,GRAV,M;TRA1;	;0001	22.29628	-166.18150 G; ;
M-DIGITAL MAGNETIC TAPES	90 024 1806		END	EOT ABC/NAV,DEPTH,GRAV,M;0015;	;0001	23.45460	-167.64000 G; ;
W-INVENTORY OF SCIENTIFIC GEAR	90 027 0415			ABC SYSTEM(NAV,MAG,GRAV);	; ;		; ;
*****DATA OR EQUIPMENT CODE = SHIPBOARD GRAVITY							
A-ANALOG PAPER ROLLS	90 003 1841		START	START OF ROLL #01	;PORT;	;0001 15.55309	-115.92225 ; ;
A-ANALOG PAPER ROLLS	90 010 2207		END	END OF ROLL #01	;0003;	;0001 25.47435	-177.16920 ; ;
A-ANALOG PAPER ROLLS	90 010 2210		START	START OF ROLL #02	;0003;	;0002 25.47240	-177.16240 ; ;

```

A-ANALOG PAPER ROLLS      90 018 1724      END      END OF ROLL #02      ;0011; ;0002 22.47940 -166.16830 ; ;
A-ANALOG PAPER ROLLS      90 018 1725      START START OF ROLL #03 ;0011; ;0003 22.48010 -166.17081 ; ;
A-ANALOG PAPER ROLLS      90 026 2006      END      END OF ROLL #03 ;TRAN; ;0003      ; ;
A-ANALOG PAPER ROLLS      90 026 2007      START START OF ROLL #04 ;TRAN; ;0004      ; ;
A-ANALOG PAPER ROLLS      90 027 1637      END      END OF ROLL #04 ;PORT; ;0004      ; ;

W-INVENTORY OF SCIENTIFIC GEAR 90 027 0415      SHIPBOARD GRAVITY      ; ; ; ;

X-OPERATION OF SCIENTIFIC GEAR 90 003 1500      ON      SYS ON: GRVTY METER ON ;PORT; ;0000 14.92136 -111.21377 ; ;
X-OPERATION OF SCIENTIFIC GEAR 90 025 0750      OFF     SYS OFF: LAB POWER LOSS ;TRAN; ;0012      ; ;
X-OPERATION OF SCIENTIFIC GEAR 90 025 0757      ON      SYS ON: POWER RSTRD ;TRAN; ;0013      ; ;
X-OPERATION OF SCIENTIFIC GEAR 90 027 0430      OFF     SYS OFF: END DATA COLL ;PORT; ;0000      ; ;

.....SYSTEM = HIGH RESOLUTION ACOUSTICS

.....DATA OR EQUIPMENT CODE = GLORIA SIDE SCAN

A-ANALOG PAPER ROLLS      90 005 0428      START START OF ROLL #01 ;TRA1; ;0001 21.34726 -159.10813 ; ;
A-ANALOG PAPER ROLLS      90 024 1800      END      END OF ROLL #01 ;0015; ;0001 23.45130 -167.62700 ; ;

```



RECORDING MEDIA      DATE AND TIME      STATUS      ACTIVITY      LINE STA- REEL      LATITUDE      LONGITUDE      R SAMP U  
 TION SAMPLE DEC DEG      DEC DEG      C DPTH N

ROLL

M-DIGITAL MAGNETIC TAPES	90 005 0428		START	START OF TAPE #01	:TRA1;	:0001	21.34726	-159.10813	; ;
M-DIGITAL MAGNETIC TAPES	90 009 0400		START	START OF TAPE #02	:0001;	:0002	26.13280	179.70150	; ;
M-DIGITAL MAGNETIC TAPES	90 009 0400		END	END OF TAPE #01	:0001;	:0001	26.13280	179.70150	; ;
M-DIGITAL MAGNETIC TAPES	90 013 0400		START	START OF TAPE #03	:0005;	:0003	26.56780	-179.93510	; ;
M-DIGITAL MAGNETIC TAPES	90 013 0400		END	END OF TAPE #02	:0005;	:0002	26.56780	-179.93510	; ;
M-DIGITAL MAGNETIC TAPES	90 017 0400		END	END OF TAPE #03	:0009;	:0003	23.65310	-170.96580	; ;
M-DIGITAL MAGNETIC TAPES	90 017 0400		START	START OF TAPE #04	:0009;	:0004	23.65310	-170.96580	; ;
M-DIGITAL MAGNETIC TAPES	90 021 0400		END	END OF TAPE #04	:0011;	:0004	25.03330	-174.71570	; ;
M-DIGITAL MAGNETIC TAPES	90 021 0400		START	START OF TAPE #05	:0011;	:0005	25.03330	-174.71570	; ;
M-DIGITAL MAGNETIC TAPES	90 024 1800		END	END OF TAPE #05	:0015;	:0005	23.45130	-167.62700	; ;

W-INVENTORY OF SCIENTIFIC GEAR 90 027 0415      GLORIA SIDE SCAN      ; ; ; ;

X-OPERATION OF SCIENTIFIC GEAR	90 005 0400	ON	SYS ON: GLORIA DEPLYD	:TRA1;	:0000	21.26722	-158.51159	; ;
X-OPERATION OF SCIENTIFIC GEAR	90 005 0428	OFF	SYS OFF: PPA REPAIRS	:TRA1;	:0001	21.34726	-159.10813	; ;
X-OPERATION OF SCIENTIFIC GEAR	90 005 0901	ON	SYS ON: PPA REPAIRED	:TRA1;	:0001	22.12763	-164.92449	; ;
X-OPERATION OF SCIENTIFIC GEAR	90 024 1800	OFF	SYS OFF:END DATA-GLOR	:0015;	:0005	23.45130	-167.62700	; ;

.....SYSTEM = STATION GRAVITY

.....DATA OR EQUIPMENT CODE = LAND TIE

O-NUMERICAL DATA OBSERVATION	90 003 1732		SAMPLE LAND TIE #1-PIER 2C/HONO;PORT;	; ;	15.35585	-114.45218	; ;
O-NUMERICAL DATA OBSERVATION	90 027 0415		SAMPLE GRAV LAND TIE/PIER 34 ;PORT;	:0000			; ;

.....SYSTEM = SHIPBOARD MAGNETICS

.....DATA OR EQUIPMENT CODE = SHIPBOARD MAGGY

A-ANALOG PAPER ROLLS	90 005 0452	START	START OF ROLL #01	:TRA1;	:0001 21.41587 -159.61948 ;
A-ANALOG PAPER ROLLS	90 007 0414	END	END OF ROLL #01	:0001;	:0001 23.98480 -172.98260 ;
A-ANALOG PAPER ROLLS	90 007 0415	START	START OF ROLL #02	:0001;	:0002 23.98560 -172.98530 ;
A-ANALOG PAPER ROLLS	90 009 0400	END	END OF ROLL #02	:0001;	:0002 26.13280 179.70150 ;
A-ANALOG PAPER ROLLS	90 009 0403	START	START OF ROLL #03	:0001;	:0003 26.13495 179.69440 ;
A-ANALOG PAPER ROLLS	90 011 0318	END	END OF ROLL #03	:0003;	:0003 25.28270 -176.47380 ;
A-ANALOG PAPER ROLLS	90 011 0319	START	START OF ROLL #04	:0003;	:0004 25.28205 -176.47150 ;
A-ANALOG PAPER ROLLS	90 013 0221	END	END OF ROLL #04	:0005;	:0004 26.49790 -179.69520 ;
A-ANALOG PAPER ROLLS	90 013 0222	START	START OF ROLL #05	:0005;	:0005 26.49850 -179.69780 ;
A-ANALOG PAPER ROLLS	90 015 0219	END	END OF ROLL #05	:0007;	:0005 26.10485 -177.44820 ;
A-ANALOG PAPER ROLLS	90 015 0220	START	START OF ROLL #06	:0007;	:0006 26.10410 -177.44580 ;
A-ANALOG PAPER ROLLS	90 017 0210	END	END OF ROLL #06	:0009;	:0006 23.72490 -171.20590 ;
A-ANALOG PAPER ROLLS	90 017 0211	START	START OF ROLL #07	:0009;	:0007 23.72430 -171.20370 ;
A-ANALOG PAPER ROLLS	90 019 0208	END	END OF ROLL #07	:0011;	:0007 22.86190 -167.43490 ;
A-ANALOG PAPER ROLLS	90 019 0209	START	START OF ROLL #08	:0011;	:0008 22.86265 -167.43736 ;
A-ANALOG PAPER ROLLS	90 021 0215	END	END OF ROLL #08	:0011;	:0008 24.95540 -174.44730 ;
A-ANALOG PAPER ROLLS	90 021 0216	START	START OF ROLL #09	:0011;	:0009 24.95620 -174.44990 ;
A-ANALOG PAPER ROLLS	90 023 0206	END	END OF ROLL #09	:0013;	:0009 23.67030 -169.21910 ;
A-ANALOG PAPER ROLLS	90 023 0207	START	START OF ROLL #10	:0013;	:0010 23.66960 -169.21670 ;
A-ANALOG PAPER ROLLS	90 024 1800	END	END OF ROLL #10	:0015;	:0010 23.45130 -167.62700 ;

RECORDING MEDIA      DATE AND TIME      STATUS      ACTIVITY      LINE STA- REEL      LATITUDE      LONGITUDE      R SAMP U  
 TION SAMPLE DEG DEG      DEC DEG      C DPTH N

W-INVENTORY OF SCIENTIFIC GEAR 90 027 0415      SHIPBOARD MAGGY      ;      ;      ;      ;      ;      ;  
 X-OPERATION OF SCIENTIFIC GEAR 90 005 0435      ON      SYS ON:DEPLOYED MAGGY ;TRA1; ;0001 21.36727 -159.25726 ; ;  
 X-OPERATION OF SCIENTIFIC GEAR 90 024 1824      OFF      SYS OFF: END DATA COL ;0015; ;0011      ;      ;

\*\*\*\*\*SYSTEM = MULTI-CHANNEL SEISMIC

\*\*\*\*\*DATA OR EQUIPMENT CODE = 2 CHANNEL AIRGUN

A-ANALOG PAPER ROLLS	90 005 1935	START	START OF ROLL #01	;TRA1;	;0001 22.49795 -167.88900	; ;
A-ANALOG PAPER ROLLS	90 005 1940	START	START OF ROLL #01	;TRA1;	;0001 22.49880 -167.90020	; ;
A-ANALOG PAPER ROLLS	90 006 2004	END	END OF ROLL #01	;0001;	;0001 23.59760 -171.67380	; ;
A-ANALOG PAPER ROLLS	90 006 2008	START	START OF ROLL #02	;0001;	;0002 23.60100 -171.68320	; ;
A-ANALOG PAPER ROLLS	90 007 2012	END	END OF ROLL #02	;0001;	;0002 24.69980 -175.42400	; ;
A-ANALOG PAPER ROLLS	90 007 2014	START	START OF ROLL #03	;0001;	;0003 24.70110 -175.42920	; ;
A-ANALOG PAPER ROLLS	90 008 2022	END	END OF ROLL #03	;0001;	;0003 25.81240 -179.21020	; ;
A-ANALOG PAPER ROLLS	90 008 2024	START	START OF ROLL #04	;0001;	;0004 25.81420 -179.21530	; ;
A-ANALOG PAPER ROLLS	90 009 1520	END	END OF ROLL #04	;0002;	;0004 26.79470 178.26750	; ;
A-ANALOG PAPER ROLLS	90 009 1525	START	START OF ROLL #05	;0003;	;0005 26.80445 178.26980	; ;
A-ANALOG PAPER ROLLS	90 010 2011	END	END OF ROLL #05	;0003;	;0005 25.55675 -177.43990	; ;
A-ANALOG PAPER ROLLS	90 010 2013	START	START OF ROLL #06	;0003;	;0006 25.55525 -177.43500	; ;
A-ANALOG PAPER ROLLS	90 011 1631	END	END OF ROLL #06	;0003;	;0006 24.75415 -174.64890	; ;
A-ANALOG PAPER ROLLS	90 011 1636	START	START OF ROLL #07	;0004;	;0007 24.76230 -174.64700	; ;
A-ANALOG PAPER ROLLS	90 012 2009	END	END OF ROLL #07	;0005;	;0007 26.20105 -178.68140	; ;
A-ANALOG PAPER ROLLS	90 012 2011	START	START OF ROLL #08	;0005;	;0008 26.20270 -178.68690	; ;
A-ANALOG PAPER ROLLS	90 013 1546	END	END OF ROLL #08	;0005;	;0008 27.13230 178.11720	; ;
A-ANALOG PAPER ROLLS	90 013 1551	START	START OF ROLL #09	;0006;	;0009 27.13935 178.10610	; ;
A-ANALOG PAPER ROLLS	90 014 2010	END	END OF ROLL #09	;0007;	;0009 26.37870 -178.34010	; ;
A-ANALOG PAPER ROLLS	90 014 2011	START	START OF ROLL #10	;0007;	;0010 26.37790 -178.33750	; ;
A-ANALOG PAPER ROLLS	90 016 0009	END	END OF ROLL #10	;0008;	;0010 24.82015 -174.84590	; ;

A-ANALOG PAPER ROLLS	90 016 0015	START	START OF ROLL #11	;0009;	;0011	24.80965	-174.84610	;
A-ANALOG PAPER ROLLS	90 016 2013	END	END OF ROLL #11	;0009;	;0011	23.95020	-171.97530	;
A-ANALOG PAPER ROLLS	90 016 2016	START	START OF ROLL #12	;0009;	;0012	23.94780	-171.96910	;
A-ANALOG PAPER ROLLS	90 017 1215	END	END OF ROLL #12	;0009;	;0012	23.32615	-169.86830	;
A-ANALOG PAPER ROLLS	90 017 1223	START	START OF ROLL #13	;0009;	;0013	23.32040	-169.84950	;
A-ANALOG PAPER ROLLS	90 018 1503	END	END OF ROLL #13	;0009;	;0013	22.20565	-166.12305	;
A-ANALOG PAPER ROLLS	90 018 1507	START	START OF ROLL #14	;0010;	;0014	22.20775	-166.11566	;
A-ANALOG PAPER ROLLS	90 019 2107	END	END OF ROLL #14	;0011;	;0014	23.69080	-170.22470	;
A-ANALOG PAPER ROLLS	90 019 2109	START	START OF ROLL #15	;0011;	;0015	23.69235	-170.22980	;
A-ANALOG PAPER ROLLS	90 021 0424	END	END OF ROLL #15	;0011;	;0015	25.05180	-174.77600	;
A-ANALOG PAPER ROLLS	90 021 0428	START	START OF ROLL #16	;0012;	;0016	25.05680	-174.78460	;
A-ANALOG PAPER ROLLS	90 021 2027	END	END OF ROLL #16	;0013;	;0016	24.91310	-173.43860	;
A-ANALOG PAPER ROLLS	90 021 2030	START	START OF ROLL #17	;0013;	;0017	24.91100	-173.43100	;
A-ANALOG PAPER ROLLS	90 022 2010	END	END OF ROLL #17	;0013;	;0017	23.90640	-170.04550	;
A-ANALOG PAPER ROLLS	90 022 2017	START	START OF ROLL #18	;0013;	;0018	23.90090	-170.02900	;
A-ANALOG PAPER ROLLS	90 023 2014	END	END OF ROLL #18	;0013;	;0018	22.89010	-166.59711	;
A-ANALOG PAPER ROLLS	90 023 2016	START	START OF ROLL #19	;0013;	;0019	22.88850	-166.59241	;
A-ANALOG PAPER ROLLS	90 024 0146	END	END OF ROLL #19	;0013;	;0019	22.65780	-165.82190	;
A-ANALOG PAPER ROLLS	90 024 0148	START	START OF ROLL #20	;0014;	;0020	22.65770	-165.81700	;
A-ANALOG PAPER ROLLS	90 024 1806	END	END OF ROLL #01	;0015;	;0001	23.45460	-167.64000	;
A-ANALOG PAPER ROLLS	90 024 1806	END	END OF ROLL #20	;0015;	;0020	23.45460	-167.64000	;

RECORDING MEDIA      DATE AND TIME      STATUS      ACTIVITY      LINE STA- REEL      LATITUDE      LONGITUDE      R SAMP U  
 TION SAMPLE DEC DEG      DEC DEG      C DPTH N

ROLL

M-DIGITAL MAGNETIC TAPES	90 005 1935	START	START OF TAPE #01	;TRA1;	;0001	22.49795	-167.88900	; ;
M-DIGITAL MAGNETIC TAPES	90 005 2043	END	END OF TAPE #01	;TRA1;	;0001	22.51855	-168.06080	; ;
M-DIGITAL MAGNETIC TAPES	90 005 2045	START	START OF TAPE #02	;0001;	;0002	22.52005	-168.06580	; ;
M-DIGITAL MAGNETIC TAPES	90 006 0456	END	END OF TAPE #02	;0001;	;0002	22.89360	-169.31560	; ;
M-DIGITAL MAGNETIC TAPES	90 006 0457	START	START OF TAPE #03	;0001;	;0003	22.89435	-169.31810	; ;
M-DIGITAL MAGNETIC TAPES	90 006 1306	END	END OF TAPE #03	;0001;	;0003	23.27360	-170.59000	; ;
M-DIGITAL MAGNETIC TAPES	90 006 1307	START	START OF TAPE #04	;0001;	;0004	23.27430	-170.59240	; ;
M-DIGITAL MAGNETIC TAPES	90 006 2118	END	END OF TAPE #04	;0001;	;0004	23.65050	-171.86740	; ;
M-DIGITAL MAGNETIC TAPES	90 006 2118	START	START OF TAPE #05	;0001;	;0005	23.65050	-171.86740	; ;
M-DIGITAL MAGNETIC TAPES	90 007 0529	END	END OF TAPE #05	;0001;	;0005	24.04405	-173.18030	; ;
M-DIGITAL MAGNETIC TAPES	90 007 0530	START	START OF TAPE #06	;0001;	;0006	24.04480	-173.18290	; ;
M-DIGITAL MAGNETIC TAPES	90 007 1340	END	END OF TAPE #06	;0001;	;0006	24.41910	-174.45230	; ;
M-DIGITAL MAGNETIC TAPES	90 007 1341	START	START OF TAPE #07	;0001;	;0007	24.41985	-174.45500	; ;
M-DIGITAL MAGNETIC TAPES	90 007 2151	START	START OF TAPE #08	;0001;	;0008	24.76705	-175.68020	; ;
M-DIGITAL MAGNETIC TAPES	90 007 2151	END	END OF TAPE #07	;0001;	;0007	24.76705	-175.68020	; ;
M-DIGITAL MAGNETIC TAPES	90 007 2214	END	EOT #8	;0001;	;0008	24.78470	-175.73990	; ;
M-DIGITAL MAGNETIC TAPES	90 007 2218	START	START OF TAPE #09	;0001;	;0009	24.78750	-175.75010	; ;
M-DIGITAL MAGNETIC TAPES	90 008 0629	END	END OF TAPE #09	;0001;	;0009	25.17335	-177.01470	; ;
M-DIGITAL MAGNETIC TAPES	90 008 0630	START	START OF TAPE #10	;0001;	;0010	25.17410	-177.01730	; ;
M-DIGITAL MAGNETIC TAPES	90 008 1440	END	END OF TAPE #10	;0001;	;0010	25.55420	-178.31370	; ;
M-DIGITAL MAGNETIC TAPES	90 008 1441	START	START OF TAPE #11	;0001;	;0011	25.55490	-178.31630	; ;
M-DIGITAL MAGNETIC TAPES	90 008 2254	END	END OF TAPE #11	;0001;	;0011	25.92860	-179.59790	; ;
M-DIGITAL MAGNETIC TAPES	90 008 2255	START	START OF TAPE #12	;0001;	;0012	25.92930	-179.60030	; ;
M-DIGITAL MAGNETIC TAPES	90 009 0703	END	END OF TAPE #12	;0001;	;0012	26.25955	179.26700	; ;
M-DIGITAL MAGNETIC TAPES	90 009 0703	START	START OF TAPE #13	;0001;	;0013	26.25955	179.26700	; ;
M-DIGITAL MAGNETIC TAPES	90 009 1235	END	END OF TAPE #13	;0001;	;0013	26.48195	178.50120	; ;
M-DIGITAL MAGNETIC TAPES	90 009 1310	START	START OF TAPE #14	;0002;	;0014	26.53910	178.43810	; ;
M-DIGITAL MAGNETIC TAPES	90 009 1520	END	END OF TAPE #14	;0002;	;0014	26.79470	178.26750	; ;
M-DIGITAL MAGNETIC TAPES	90 009 1531	START	START OF TAPE #15	;0003;	;0015	26.80705	178.28340	; ;
M-DIGITAL MAGNETIC TAPES	90 009 2343	START	START OF TAPE #16	;0003;	;0016	26.43815	179.56270	; ;
M-DIGITAL MAGNETIC TAPES	90 009 2343	END	END OF TAPE #15	;0003;	;0015	26.43815	179.56270	; ;
M-DIGITAL MAGNETIC TAPES	90 010 0753	START	START OF TAPE #17	;0003;	;0017	26.09075	-179.25570	; ;

M-DIGITAL MAGNETIC TAPES	90 010 0753	END	END OF TAPE #16	;0003; ;0016 26.09075 -179.25570 ; ;
M-DIGITAL MAGNETIC TAPES	90 010 1604	END	END OF TAPE #17	;0003; ;0017 25.74200 -178.06430 ; ;
M-DIGITAL MAGNETIC TAPES	90 010 1605	START	START OF TAPE #18	;0003; ;0018 25.74125 -178.06160 ; ;
M-DIGITAL MAGNETIC TAPES	90 011 0015	END	END OF TAPE #18	;0003; ;0018 25.39015 -176.88370 ; ;
M-DIGITAL MAGNETIC TAPES	90 011 0016	START	START OF TAPE #19	;0003; ;0019 25.38960 -176.88130 ; ;
M-DIGITAL MAGNETIC TAPES	90 011 0827	END	END OF TAPE #19	;0003; ;0019 25.06790 -175.74540 ; ;
M-DIGITAL MAGNETIC TAPES	90 011 0827	START	START OF TAPE #20	;0003; ;0020 25.06790 -175.74540 ; ;
M-DIGITAL MAGNETIC TAPES	90 011 1625	END	END OF TAPE #20	;0003; ;0020 24.75030 -174.65780 ; ;
M-DIGITAL MAGNETIC TAPES	90 011 1641	START	START OF TAPE #21	;0004; ;0021 24.77240 -174.65020 ; ;
M-DIGITAL MAGNETIC TAPES	90 011 1836	END	END OF TAPE #21	;0004; ;0021 25.02690 -174.75190 ; ;
M-DIGITAL MAGNETIC TAPES	90 011 1844	START	START OF TAPE #22	;0005; ;0022 25.04440 -174.76170 ; ;
M-DIGITAL MAGNETIC TAPES	90 012 0255	END	END OF TAPE #22	;0005; ;0022 25.41020 -175.98910 ; ;
M-DIGITAL MAGNETIC TAPES	90 012 0256	START	START OF TAPE #23	;0005; ;0023 25.41090 -175.99150 ; ;
M-DIGITAL MAGNETIC TAPES	90 012 1106	END	END OF TAPE #23	;0005; ;0023 25.78390 -177.26250 ; ;
M-DIGITAL MAGNETIC TAPES	90 012 1106	START	START OF TAPE #24	;0005; ;0024 25.78390 -177.26250 ; ;
M-DIGITAL MAGNETIC TAPES	90 012 1918	END	END OF TAPE #24	;0005; ;0024 26.16000 -178.53940 ; ;
M-DIGITAL MAGNETIC TAPES	90 012 1918	START	START OF TAPE #25	;0005; ;0025 26.16000 -178.53940 ; ;
M-DIGITAL MAGNETIC TAPES	90 013 0329	END	END OF TAPE #25	;0005; ;0025 26.54545 -179.86120 ; ;
M-DIGITAL MAGNETIC TAPES	90 013 0330	START	START OF TAPE #26	;0005; ;0026 26.54620 -179.86360 ; ;
M-DIGITAL MAGNETIC TAPES	90 013 1140	END	END OF TAPE #26	;0005; ;0026 26.93360 178.80850 ; ;
M-DIGITAL MAGNETIC TAPES	90 013 1140	START	START OF TAPE #27	;0005; ;0027 26.93360 178.80850 ; ;
M-DIGITAL MAGNETIC TAPES	90 013 1546	END	END OF TAPE #27	;0005; ;0027 27.13230 178.11720 ; ;

RECORDING MEDIA      DATE AND TIME      STATUS      ACTIVITY      LINE STA- REEL      LATITUDE      LONGITUDE      R SAMP      U  
 TION SAMPLE DEC DEG      DEC DEG      C DPTH N

RECORDING MEDIA	DATE AND TIME	STATUS	ACTIVITY	LINE STA- REEL	LATITUDE	LONGITUDE	R SAMP	U
M-DIGITAL MAGNETIC TAPES	90 005 1935	START	START OF TAPE #01	:TRA1;	:0001	22.49795	-167.88900	;
M-DIGITAL MAGNETIC TAPES	90 005 2043	END	END OF TAPE #01	:TRA1;	:0001	22.51855	-168.06080	;
M-DIGITAL MAGNETIC TAPES	90 005 2045	START	START OF TAPE #02	:0001;	:0002	22.52005	-168.06580	;
M-DIGITAL MAGNETIC TAPES	90 006 0456	END	END OF TAPE #02	:0001;	:0002	22.89360	-169.31560	;
M-DIGITAL MAGNETIC TAPES	90 006 0457	START	START OF TAPE #03	:0001;	:0003	22.89435	-169.31810	;
M-DIGITAL MAGNETIC TAPES	90 006 1306	END	END OF TAPE #03	:0001;	:0003	23.27360	-170.59000	;
M-DIGITAL MAGNETIC TAPES	90 006 1307	START	START OF TAPE #04	:0001;	:0004	23.27430	-170.59240	;
M-DIGITAL MAGNETIC TAPES	90 006 2118	END	END OF TAPE #04	:0001;	:0004	23.65050	-171.86740	;
M-DIGITAL MAGNETIC TAPES	90 006 2118	START	START OF TAPE #05	:0001;	:0005	23.65050	-171.86740	;
M-DIGITAL MAGNETIC TAPES	90 007 0529	END	END OF TAPE #05	:0001;	:0005	24.04405	-173.18030	;
M-DIGITAL MAGNETIC TAPES	90 007 0530	START	START OF TAPE #06	:0001;	:0006	24.04480	-173.18290	;
M-DIGITAL MAGNETIC TAPES	90 007 1340	END	END OF TAPE #06	:0001;	:0006	24.41910	-174.45230	;
M-DIGITAL MAGNETIC TAPES	90 007 1341	START	START OF TAPE #07	:0001;	:0007	24.41985	-174.45500	;
M-DIGITAL MAGNETIC TAPES	90 007 2151	START	START OF TAPE #08	:0001;	:0008	24.76705	-175.68020	;
M-DIGITAL MAGNETIC TAPES	90 007 2151	END	END OF TAPE #07	:0001;	:0007	24.76705	-175.68020	;
M-DIGITAL MAGNETIC TAPES	90 007 2214	END	EOT #8	:0001;	:0008	24.78470	-175.73990	;
M-DIGITAL MAGNETIC TAPES	90 007 2218	START	START OF TAPE #09	:0001;	:0009	24.78750	-175.75010	;
M-DIGITAL MAGNETIC TAPES	90 008 0629	END	END OF TAPE #09	:0001;	:0009	25.17335	-177.01470	;
M-DIGITAL MAGNETIC TAPES	90 008 0630	START	START OF TAPE #10	:0001;	:0010	25.17410	-177.01730	;
M-DIGITAL MAGNETIC TAPES	90 008 1440	END	END OF TAPE #10	:0001;	:0010	25.55420	-178.31370	;
M-DIGITAL MAGNETIC TAPES	90 008 1441	START	START OF TAPE #11	:0001;	:0011	25.55490	-178.31630	;
M-DIGITAL MAGNETIC TAPES	90 008 2254	END	END OF TAPE #11	:0001;	:0011	25.92860	-179.59790	;
M-DIGITAL MAGNETIC TAPES	90 008 2255	START	START OF TAPE #12	:0001;	:0012	25.92930	-179.60030	;
M-DIGITAL MAGNETIC TAPES	90 009 0703	END	END OF TAPE #12	:0001;	:0012	26.25955	179.26700	;
M-DIGITAL MAGNETIC TAPES	90 009 0703	START	START OF TAPE #13	:0001;	:0013	26.25955	179.26700	;
M-DIGITAL MAGNETIC TAPES	90 009 1235	END	END OF TAPE #13	:0001;	:0013	26.48195	178.50120	;
M-DIGITAL MAGNETIC TAPES	90 009 1310	START	START OF TAPE #14	:0002;	:0014	26.53910	178.43810	;
M-DIGITAL MAGNETIC TAPES	90 009 1520	END	END OF TAPE #14	:0002;	:0014	26.79470	178.26750	;
M-DIGITAL MAGNETIC TAPES	90 009 1531	START	START OF TAPE #15	:0003;	:0015	26.80705	178.28340	;
M-DIGITAL MAGNETIC TAPES	90 009 2343	START	START OF TAPE #16	:0003;	:0016	26.43815	179.56270	;
M-DIGITAL MAGNETIC TAPES	90 009 2343	END	END OF TAPE #15	:0003;	:0015	26.43815	179.56270	;
M-DIGITAL MAGNETIC TAPES	90 010 0753	START	START OF TAPE #17	:0003;	:0017	26.09075	-179.25570	;



M-DIGITAL MAGNETIC TAPES	90 019 0112	START START OF TAPE #45	;0011; ;0045 22.81960 -167.29761 ; ;
M-DIGITAL MAGNETIC TAPES	90 019 0924	END END OF TAPE #45	;0011; ;0045 23.18240 -168.50230 ; ;
M-DIGITAL MAGNETIC TAPES	90 019 0924	START START OF TAPE #46	;0011; ;0046 23.18240 -168.50230 ; ;
M-DIGITAL MAGNETIC TAPES	90 019 1735	END END OF TAPE #46	;0011; ;0046 23.53840 -169.68980 ; ;
M-DIGITAL MAGNETIC TAPES	90 019 1736	START START OF TAPE #47	;0011; ;0047 23.53910 -169.69240 ; ;
M-DIGITAL MAGNETIC TAPES	90 020 0146	END END OF TAPE #47	;0011; ;0047 23.89550 -170.88630 ; ;
M-DIGITAL MAGNETIC TAPES	90 020 0147	START START OF TAPE #48	;0011; ;0048 23.89615 -170.88870 ; ;
M-DIGITAL MAGNETIC TAPES	90 020 0957	START START OF TAPE #49	;0011; ;0049 24.24045 -172.03910 ; ;
M-DIGITAL MAGNETIC TAPES	90 020 0957	END END OF TAPE #48	;0011; ;0048 24.24045 -172.03910 ; ;
M-DIGITAL MAGNETIC TAPES	90 020 1135	END EOT #49: MASS CMP PBLM	;0011; ;0049 24.31185 -172.28000 ; ;
M-DIGITAL MAGNETIC TAPES	90 020 1315	START START OF TAPE #50	;0011; ;0050 24.38725 -172.53260 ; ;
M-DIGITAL MAGNETIC TAPES	90 020 2021	END END OF TAPE #50	;0011; ;0050 24.67180 -173.56980 ; ;
M-DIGITAL MAGNETIC TAPES	90 020 2022	START START OF TAPE #51	;0011; ;0051 24.67240 -173.57210 ; ;
M-DIGITAL MAGNETIC TAPES	90 021 0424	END END OF TAPE #51	;0011; ;0051 25.05180 -174.77600 ; ;
M-DIGITAL MAGNETIC TAPES	90 021 0430	START START OF TAPE #52	;0012; ;0052 25.05980 -174.78830 ; ;
M-DIGITAL MAGNETIC TAPES	90 021 0801	END END OF TAPE #52	;0012; ;0052 25.39995 -175.17620 ; ;
M-DIGITAL MAGNETIC TAPES	90 021 0816	START START OF TAPE #53	;0013; ;0053 25.41690 -175.16050 ; ;
M-DIGITAL MAGNETIC TAPES	90 021 1627	END END OF TAPE #53	;0013; ;0053 25.08955 -174.02430 ; ;
M-DIGITAL MAGNETIC TAPES	90 021 1628	START START OF TAPE #54	;0013; ;0054 25.08880 -174.02190 ; ;
M-DIGITAL MAGNETIC TAPES	90 022 0039	END END OF TAPE #54	;0013; ;0054 24.75355 -172.87750 ; ;
M-DIGITAL MAGNETIC TAPES	90 022 0039	START START OF TAPE #55	;0013; ;0055 24.75355 -172.87750 ; ;
M-DIGITAL MAGNETIC TAPES	90 022 1702	END END OF TAPE #56	;0013; ;0056 24.05090 -170.49580 ; ;

RECORDING MEDIA	DATE AND TIME	STATUS	ROLL ACTIVITY	LINE STA- REEL	LATITUDE	LONGITUDE	R SAMP U
			TION SAMPLE DEC DEG	DEC DEG	C DPTH N		
M-DIGITAL MAGNETIC TAPES	90 022 1703		START OF TAPE #57	:0013;	:0057	24.05020	-170.49340 ; ;
M-DIGITAL MAGNETIC TAPES	90 022 2209		END OF TAPE #55	:0013;	:0055	23.82825	-169.76980 ; ;
M-DIGITAL MAGNETIC TAPES	90 022 2209		START OF TAPE #56	:0013;	:0056	23.82825	-169.76980 ; ;
M-DIGITAL MAGNETIC TAPES	90 023 0112		END OF TAPE #57	:0013;	:0057	23.70840	-169.34590 ; ;
M-DIGITAL MAGNETIC TAPES	90 023 0113		START OF TAPE #58	:0013;	:0058	23.70770	-169.34360 ; ;
M-DIGITAL MAGNETIC TAPES	90 023 0924		START OF TAPE #59	:0013;	:0059	23.35280	-168.15280 ; ;
M-DIGITAL MAGNETIC TAPES	90 023 0924		END OF TAPE #58	:0013;	:0058	23.35280	-168.15280 ; ;
M-DIGITAL MAGNETIC TAPES	90 023 1735		END OF TAPE #59	:0013;	:0059	23.00555	-166.98961 ; ;
M-DIGITAL MAGNETIC TAPES	90 023 1736		START OF TAPE #60	:0013;	:0060	23.00480	-166.98720 ; ;
M-DIGITAL MAGNETIC TAPES	90 023 2025		END OF TAPE #60	:0013;	:0060	22.88155	-166.57091 ; ;
M-DIGITAL MAGNETIC TAPES	90 023 2054		START OF TAPE #61	:0013;	:0061	22.86050	-166.50270 ; ;
M-DIGITAL MAGNETIC TAPES	90 024 0141		END OF TAPE #61	:0013;	:0061	22.66025	-165.83385 ; ;
M-DIGITAL MAGNETIC TAPES	90 024 0156		START OF TAPE #62	:0014;	:0062	22.66340	-165.79800 ; ;
M-DIGITAL MAGNETIC TAPES	90 024 0342		END OF TAPE #62	:0014;	:0062	22.81010	-165.56960 ; ;
M-DIGITAL MAGNETIC TAPES	90 024 0352		START OF TAPE #63	:0015;	:0063	22.82860	-165.56850 ; ;
M-DIGITAL MAGNETIC TAPES	90 024 1203		END OF TAPE #63	:0015;	:0063	23.19160	-166.76286 ; ;
M-DIGITAL MAGNETIC TAPES	90 024 1204		START OF TAPE #64	:0015;	:0064	23.19230	-166.76530 ; ;
M-DIGITAL MAGNETIC TAPES	90 024 1808		END OF TAPE #64	:0015;	:0064		;
W-INVENTORY OF SCIENTIFIC GEAR	90 027 0415		TWO CHANNEL AIR GUN	;	;		;
X-OPERATION OF SCIENTIFIC GEAR	90 005 1935	ON	SYS ON: TCAG DEPLYD	:TRA1;	:0001	22.49795	-167.88900 ; ;
X-OPERATION OF SCIENTIFIC GEAR	90 005 2127	OFF	SYS OFF:GUN LOST PRSS	:0001;	:0002	22.55165	-168.17210 ; ;
X-OPERATION OF SCIENTIFIC GEAR	90 005 2200	ON	SYS ON:AIR GUN RSTRD	:0001;	:0002	22.57680	-168.25630 ; ;
X-OPERATION OF SCIENTIFIC GEAR	90 011 2043	OFF	SYS OFF: CHG AIR GUN	:0005;	:0022	25.12040	-175.06970 ; ;
X-OPERATION OF SCIENTIFIC GEAR	90 011 2145	ON	SYS ON: AIR GUN CHGD	:0005;	:0022	25.16280	-175.22740 ; ;
X-OPERATION OF SCIENTIFIC GEAR	90 015 1857	OFF	SYS OFF: PULLING STRMR	:0007;	:0034	25.35615	-174.91260 ; ;
X-OPERATION OF SCIENTIFIC GEAR	90 016 0057	ON	SYS ON: STRMR RESTORED	:0009;	:0035	24.77695	-174.75720 ; ;
X-OPERATION OF SCIENTIFIC GEAR	90 016 2220	OFF	SYS OFF:UNKWN NOISE ON	:0009;	:0037	23.85970	-171.68890 ; ;
X-OPERATION OF SCIENTIFIC GEAR	90 016 2223	ON	SYS ON:NOISE CONTINUES	:0009;	:0037	23.85830	-171.68210 ; ;
X-OPERATION OF SCIENTIFIC GEAR	90 016 2356	OFF	SYS OFF:NOISE CONTINUES	:0009;	:0037	23.80400	-171.47420 ; ;
X-OPERATION OF SCIENTIFIC GEAR	90 017 0005	ON	SYS ON:NOISE CONTINUES	:0009;	:0037	23.79900	-171.45680 ; ;

X-OPERATION OF SCIENTIFIC GEAR	90 017 0011	OFF	SYS OFF: NOISE CONTINUES ;0009;	;0037	23.79605	-171.44710	; ;
X-OPERATION OF SCIENTIFIC GEAR	90 017 0111	ON	SYS ON: NOISE CONTINUES ;0009;	;0037	23.76200	-171.33230	; ;
X-OPERATION OF SCIENTIFIC GEAR	90 017 2013	OFF	SYS OFF: REPOSTN STRMR ;0009;	;0040	22.98800	-168.73420	; ;
X-OPERATION OF SCIENTIFIC GEAR	90 017 2017	ON	SYS ON: STRMR REPOS 50M ;0009;	;0040	22.98505	-168.72460	; ;
X-OPERATION OF SCIENTIFIC GEAR	90 020 1135	OFF	SYS OFF: MASS COMP PBLM ;0011;	;0049	24.31185	-172.28000	; ;
X-OPERATION OF SCIENTIFIC GEAR	90 020 1315	ON	SYS ON: MASS COMP RSTRD ;0011;	;0050	24.38725	-172.53260	; ;
X-OPERATION OF SCIENTIFIC GEAR	90 021 2252	OFF	SYS OFF: CHG AIR GUN ;0013;	;0054	24.82180	-173.11230	; ;
X-OPERATION OF SCIENTIFIC GEAR	90 022 0022	ON	SYS ON: AIR GUN CHGD ;0013;	;0054	24.76530	-172.91640	; ;
X-OPERATION OF SCIENTIFIC GEAR	90 023 2025	OFF	SYS OFF: PBLM MASS COMP ;0013;	;0060	22.88155	-166.57091	; ;
X-OPERATION OF SCIENTIFIC GEAR	90 023 2054	ON	SYS ON: MASS COMP RSTRD ;0013;	;0061	22.86050	-166.50270	; ;
X-OPERATION OF SCIENTIFIC GEAR	90 024 1808	OFF	SYS OFF: END DATA COLL ;0015;	;0064			; ;